



**U.S. Department of Housing and Urban Development**  
Office of Policy Development and Research

---



# ***In-Plane Shear Resistance of Insulating Concrete Form Walls***

PATH (Partnership for Advancing Technology in Housing) is a new private/public effort to develop, demonstrate, and gain widespread market acceptance for the “Next Generation” of American housing. Through the use of new or innovative technologies the goal of PATH is to improve the quality, durability, environmental efficiency, and affordability of tomorrow’s homes.

PATH, initiated jointly by the Administration and Congress, is managed and supported by the Department of Housing and Urban Development (HUD). In addition, all Federal Agencies that engage in housing research and technology development are PATH Partners, including the Departments of Energy and Commerce, as well as the Environmental Protection Agency (EPA) and the Federal Emergency Management Agency (FEMA). State and local governments and other participants from the private sector are also partners in PATH. Product manufacturers, home builders, insurance companies, and lenders represent private industry in the PATH Partnership.

To learn more about PATH, please contact:



451 7th Street, SW  
Suite B133  
Washington, DC 20410  
202-708-4250 (fax)  
e-mail: [pathnet@pathnet.org](mailto:pathnet@pathnet.org)  
website: [www.pathnet.org](http://www.pathnet.org)

# ***In-Plane Shear Resistance of Insulating Concrete Form Walls***

Prepared for:

U.S. Department of Housing and Urban Development  
Office of Policy Development and Research  
Washington, DC

Portland Cement Association  
Skokie, IL

Prepared by:

NAHB Research Center, Inc.  
Upper Marlboro, MD

Contract H-21172CA

April 2001



## **Acknowledgments**

The NAHB Research Center, Inc., expresses great appreciation to the sponsors of this work in view of its relevance to more efficient design and construction of residential buildings using insulating concrete forms. William Freeborne of the U.S. Department of Housing and Urban Development, Office of Policy Development and Research, is also recognized for his contribution to this program. Special recognition is given to the following manufacturers who provided materials for tests conducted in this project:

AAB Building Systems Inc., Cobourg, Ontario  
Reddi-Form, Inc., Oakland, NJ  
Reward Walls, Omaha, NE

The Research Center personnel involved in this work include:

Shawn McKee, Principal Investigator  
Jay Crandell, P.E., Technical Reviewer  
Brian Bramel, Ph.D., P.E., Technical Support  
Lisa Zimmerman, Administrative Support  
Brian Adgate, Laboratory Support  
Anthony Osborne, Laboratory Support

Special thanks to the ICF builder who helped construct the test specimens:  
Frank Ruff, Topcraft Homes, Davidsonville, MD

## **Disclaimer**

The work that provided the basis for this publication was supported by funding under a grant with the U.S. Department of Housing and Urban Development. The substance and findings of the work are dedicated to the public. The author and publisher are solely responsible for the accuracy of the statements and interpretations contained in this publication. Such interpretations do not necessarily reflect the views of the Government.

*The NAHB Research Center, Inc. is a not-for-profit subsidiary of the National Association of Home Builders (NAHB). The NAHB has 200,000 members, including 60,000 builders who build more than 80 percent of new American homes. NAHB Research Center, Inc. conducts research, analysis, and demonstration programs in all areas relating to home building, and carries out extensive programs of information dissemination and interchange among members of the industry and between the industry and the public.*

## Table of Contents

Acknowledgments.....	ii
List of Tables .....	iv
List of Figures .....	v
Introduction.....	1
Background.....	1
ICF Wall Design for Parallel (In-Plane) Shear .....	5
Experimental Program .....	8
Test Procedure .....	12
Test Results and Discussion.....	13
<i>General Observations of Wall Behavior</i> .....	13
<i>Force-Displacement Response</i> .....	21
<i>Initial Stiffness</i> .....	25
<i>Energy Dissipated</i> .....	25
Design Evaluation.....	26
<i>Flat Specimens</i> .....	26
<i>Waffle – Grid Specimens</i> .....	27
<i>Screen – Grid Specimens</i> .....	28
Investigation of an Empirical Design Method .....	29
Design Methodology.....	31
Conclusions.....	31
Recommendations.....	32
References.....	33
Appendix A – Example Calculations.....	36

## List of Tables

Table 1 - Specimen Details .....	8
Table 2 - Concrete Mix Data .....	10
Table 3 - Concrete Compression Tests .....	11
Table 4 - Rebar Tension Tests .....	12
Table 5 - Test Observations for the Flat Shear Wall Specimens .....	13
Table 6 - Test Observations for the Waffle-Grid Shear Wall Specimens .....	16
Table 7 - Test Observations for the Screen-Grid Shear Wall Specimens .....	19
Table 8 - Force-Displacement Data Summary from Testing .....	21
Table 9 - Comparison of Actual to Effective Stiffness .....	25
Table 10 - Tested vs. Predicted Shear Capacities for Flat Test Specimens using Model 1 and Model 2 .....	26
Table 11 - Tested vs. Predicted Shear Capacities for Waffle-Grid Specimens using Model 1 and Model 2 .....	27
Table 12 - Effective Wall Thickness for 6 in Waffle-Grid Specimens .....	27
Table 13 - Tested vs. Predicted Shear Capacities for Screen-Grid Specimens using Model 1 and Model 2 .....	28
Table 14 - Effective Wall Thickness for 6 in Screen-Grid Specimens .....	28
Table 15 - Effective Wall Thickness from Data Published by PCA .....	29

## List of Figures

Figure 1 - Diagrams and Dimensions of ICF Systems Used to Construct the Shear Wall Specimens.....	9
Figure 2 - NAHB Research Center's Shear Wall Testing Facility.....	12
Figure 3 - Typical Hairline Cracking at the Corners of the Window Opening.....	14
Figure 4 - Failure Mechanism of Flat No. 2 Wall Specimen.....	14
Figure 5 - Failure Mechanism of Flat No. 3 Wall Specimen.....	15
Figure 6 - Final Lateral Displacement of Flat No. 3 Wall Specimen.....	15
Figure 7 - Failure Mechanism of Waffle No. 1 Wall Specimen.....	17
Figure 8 - Typical Hairline Cracking at the Corner of the Window Opening (Waffle No. 2).....	17
Figure 9 - Failure Mechanism of Waffle No. 2 Wall Specimen.....	18
Figure 10 - Final Lateral Displacement of Waffle No. 3 Wall Specimen.....	18
Figure 11 - Failure Mechanism of Screen No. 1 Wall Specimen.....	19
Figure 12 - Failure Mechanism of Screen No. 2 Wall Specimen.....	20
Figure 13 - Final Lateral Displacement of Screen No. 3 Wall Specimen.....	20
Figure 14 - Force-Displacement Response for the Flat ICF Shear Wall Specimens.....	22
Figure 15 - Force-Displacement Response for the Waffle-Grid ICF Shear Wall Specimens.....	22
Figure 16 - Force-Displacement Response for the Screen-Grid ICF Shear Wall Specimens.....	23
Figure 17 - Force-Displacement Response for the 4ft x 8ft ICF Shear Wall Specimens.....	23
Figure 18 - Force-Displacement Response for the 12ft x 8ft with Window Opening ICF Shear Wall Specimens.....	24
Figure 19 - Force-Displacement Response for the 12ft x 8ft with Garage Opening ICF Shear Wall Specimens.....	24
Figure 20 - Ultimate Capacity vs. Opening Area Ratio.....	30



## Introduction

The efficient use of shear walls in residential construction subjected to wind and seismic loading is of great interest to designers and builders of homes in high hazard areas of the United States. Shear walls are the primary lateral force resisting system in residential construction. There has been considerable research aimed at optimizing the design of light-framed shear walls (wood and cold-formed steel) in recent years. For relatively new types of wall systems, such as Insulating Concrete Form (ICF) wall construction, the technical information available is limited. There is a need to confirm or improve the use of traditional concrete shear wall design methods particularly in the context of ICF systems and residential construction practices. Thus, inefficiencies that result in conservative (uneconomical) or unconservative (unsafe) applications may be avoided.

A research program was initiated at the NAHB Research Center to study the structural performance of ICF walls when subjected to in-plane shear loading. An experimental study was designed to determine the influence of the following factors on the in-plane shear strength of ICF walls: (1) height-to-length aspect ratio of shear wall segments, (2) openings for windows and doors, and (3) the current minimal reinforcement details provided by the *Prescriptive Method for Insulating Concrete Forms in Residential Construction (Prescriptive Method)* [1]. The main goal of this study was to confirm and improve methods of evaluating the in-plane shear capacity of ICF walls. This information is intended to improve the shear wall design and construction guidance found in the *Prescriptive Method* [1] and the *International Residential Code* [2].

## Background

Reinforced concrete shear walls can resist a large portion of the shear due to lateral loads on buildings. However, failures of reinforced concrete walls are not necessarily dominated by shear deformations. The balance between shear and flexure loading has a very significant role in overall deformation and strength characteristics. Walls with a height-to-length aspect ratio of more than about 2.0 possess flexure dominated deformational characteristics while walls with aspect ratios less than 2.0 are influenced more by the presence of high shear loads [3]. However, this rule may not apply to lightly reinforced concrete walls as found in the *Prescriptive Method* [1] and the *International Residential Code* [2].

The use of reinforced concrete structural walls is common for resisting lateral loads imposed by wind and earthquakes. In practice there are two different types of structural concrete walls: cantilever shear walls and framed shear walls. Cantilever shear walls act as cantilever beams and are connected to the rest of the structure by floor diaphragms through which horizontal forces are transmitted to the wall. The design of cantilever shear walls is usually governed by flexural behavior. The design philosophy is to ensure a ductile flexural failure where the tensile steel in the boundary element reaches yielding before the web fails in shear.

The framed shear wall panel is considered to be an element that stiffens the shear resistance of a plane frame. A framed shear wall is considered as part of the overall frame system except that it receives a larger portion of the shear loads due to its greater stiffness. However, it is not considered to receive a large overturning moment as in the cantilever shear wall because it is constrained by the surrounding frame. It is essentially an in-fill wall that is designed to resist shear. Consequently, the framed shear wall behaves differently than does a cantilever wall – the

predominant action is shear [4]. The design of ICF walls for residential construction more closely resembles the cantilever shear wall model.

The ultimate strength capacity of an individual shear wall element is a function of the material strengths, the applied loading, and the geometry of the wall, including the amount of reinforcement and the reinforcement detailing. Failure modes resulting from in-plane loads include shear friction, diagonal shear cracking, flexural reinforcement yielding, and web crushing. Other less desirable failure modes include reinforcement pullout (reinforcement development length failure) or concrete failure as a result of overturning tensile forces.

In the shear friction mode, the wall responds linearly until a horizontal crack forms, typically at the base of the wall, parallel to the applied load. At this point, the wall rotates as a rigid body, causing the reinforcing steel to yield. Because of the progressive yielding, when the loading is reversed, sliding displacement occurs along the horizontal crack. For this mode of failure to occur, a horizontal crack must form at the base of the wall before diagonal shear cracking forms. This mode typically controls the capacity of lightly reinforced low-rise shear walls [5].

If the shear walls have reinforcement in excess of the minimum required by ACI-318 [6] and a height-to-length aspect ratio between 0.5 and 1.0, testing reveals diagonal shear cracking is the predominant failure mode. These cracks begin at the base of the wall nearest the applied load and occur at the same time that flexural cracks are noticed near the tension face. Diagonal cracks continue to form under increasing load and are eventually accompanied by yielding of the vertical reinforcement [5].

Shear forces caused by lateral loads are accompanied by a moment applied in the plane of the wall. The presence of these moments requires that a flexural failure mode also be examined. The failure mode can result in either a crushing of the compression zone concrete (if the wall is heavily reinforced or constrained from overturning) or yielding of the tension bars. Typically, crushing of the concrete in the web is not considered because the percentages of reinforcement are kept below a balanced design value ensuring that the tension reinforcement will yield before crushing can occur [7]. To assess the strength of a shear wall, the capacity to withstand these various failure modes must be evaluated using mechanics-based expressions that have been empirically validated or modified.

Experimental research toward the behavior of reinforced concrete walls is concentrated mainly in the U.S., Japan, and New Zealand, with some more recent contributions from Europe. The Portland Cement Association (PCA) was among the pioneers in the field in the 1970's. Cardenas et al. tested thirteen walls at a scale of 1:2 under monotonic loading [5]. Osterle et al. conducted an extensive test program on walls of scale 1:3 with the ductility, energy dissipation, and strength of the walls as the primary aim of the investigation [7]. Flanged, barbell, and rectangular sections were investigated. The first two types of construction were found to be susceptible to web crushing while the rectangular sections experienced out of plane instability. Both studies concluded that shear reinforcement supplied to resist the expected maximum flexural response is sufficient to avoid shear failure. Any additional shear reinforcement had little effect on the shear stiffness. It was also reported that closed hoop reinforcement, typically used to improve the torsional resistance, improved the elastic shear behavior of the reinforced concrete walls. By

applying uniform axial loads of 10-percent of the ultimate compression strength, the axial loading was found to have a beneficial effect on the flexural capacity [7].

Relatively little testing has been done to evaluate the performance of reinforced concrete walls with openings. Current building codes, such as the *Uniform Building Code* [8], include provisions for the design of symmetrical and unsymmetrical solid concrete walls; however, it is often necessary to provide openings in the walls for doors and windows. If the openings are small relative to the wall dimensions, it may be reasonable to neglect the effects of the openings [9]. In many cases, the opening is relatively large or is located in a critical region where inelastic deformations are expected. In such cases, the influence of the opening on the overall wall behavior must be evaluated.

Since current U.S. codes do not provide exact design guidelines for walls with openings, considerable engineering judgement is required. In general, the influence of the opening on the flexural and shear strength, as well as the design requirements, should be considered. If the opening is near the middle of the wall, it will decrease the moment capacity of the wall only slightly; however, the shear strength may be significantly reduced. In contrast, an opening near a wall boundary may impact both the moment and shear strengths. Recent research of reinforced concrete shear walls with openings is discussed below.

Research conducted by Ali and Wight on one-quarter scale slender walls with staggered openings revealed the walls were vulnerable to shear compression failure in the narrow wall segment when the opening at the base was near the wall boundary [10]. One specimen was tested without openings and excellent behavior at large drift ratios was observed, even though only moderate detailing of the boundary zones was provided compared with ACI 318-95 requirements [10]. This improved behavior was explained using a displacement design approach [11]. Recently published research on the behavior of slender walls has shown that a displacement design approach provides a versatile design methodology [9] [11]. The procedure involves comparing the strain capacity of the wall with the estimated strains imposed on the wall as a result of a design earthquake. In general, providing additional transverse boundary reinforcement can increase the strain capacity of a wall. Thus, rather than providing an arbitrary amount of confining reinforcement at the wall boundaries, confinement is selected based on the deformation or strain demand. However, this method is not considered an efficient design approach for residential construction due to the increased complexity of reinforcement details required at the boundary elements.

Taylor et al. conducted two one-quarter scale tests to determine the effects of openings at the base of slender reinforced concrete walls [9]. The walls were 12 ft (3.66 m) high by 4 ft (1.22 m) long resulting in a height-to-length aspect ratio of 3.0. A 20 in (508 mm) high by 9 in (229 mm) long opening was provided at the base of each specimen located 3.5 in (89 mm) from the edge of the wall. One specimen had a rectangular cross section and one had a barbell cross-section. A constant axial load of approximately  $0.10f'_cA_g$  was applied to the walls for the duration of each test. This level of axial load was used to represent the dead load in a typical moderate-rise building. The research concluded that slender structural walls with openings can exhibit stable behavior and significant ductility, even for cases when the opening is in the flexural compression zone. The large opening at the base did not significantly influence the behavior or strength of the wall compared to the walls without openings. Vertical cracks above the door opening indicate that the reinforcement in this location was effective in providing a load path around the opening.

Lefas et al. tested 13 reinforced concrete shear walls with a constant thickness and a height-to-length aspect ratio ranging between 1.0 and 2.0. The vertical and horizontal reinforcement consisted of high tensile strength deformed bars. Additional horizontal reinforcement in the form of stirrups confined the wall edges. Three levels of constant axial load were applied in the testing program; they corresponded to  $0.0 f'_c A_g$ ,  $0.1 f'_c A_g$ , and  $0.2 f'_c A_g$ . These load levels were considered to represent the amount of axial load at the base of the wall of a single story, a medium-height, and a high-rise building, respectively [12].

Failure of the walls occurred due to the nearly vertical splitting of the compression zone in the region of the inclined or deepest flexural crack, followed by splitting of the whole compressive zone. The failure region was more extensive with decreasing height-to-length aspect ratio and increasing axial load [12].

The ultimate shear capacity of the specimens with axial loads equal to  $0.1 f'_c A_g$ , and  $0.2 f'_c A_g$  was higher than that of the walls subjected to shear load only by about 25 and 30 percent, respectively. The axial load also reduced the value of the horizontal displacement at peak load. Differences in compressive concrete strength as high as 35 percent resulted in almost negligible variation in wall strength. This may indicate that strength and deformation characteristics of the walls are not significantly affected by variability in concrete strength [12].

The observed maximum shear capacity sustained by the walls substantially exceeded the calculated flexural and shear capacities defined by ACI 318. Although ACI 318 provisions indicated a ductile flexural failure mode, the specimens actually exhibited a shear failure mode while remaining ductile. Specimens that utilized about half of the horizontal web reinforcement required by ACI 318 to safeguard against a non-ductile shear failure also failed by shear in a ductile manner. Such behaviors indicated that significant reductions in the horizontal web reinforcement does not have a significant effect on shear capacity [12].

Research for the Portland Cement Association investigated the in-plane shear resistance of various types of wall construction commonly used in residential construction. This study included three concrete shear walls with a height-to-length aspect ratio of 2.0 constructed with the major ICF system types (flat, waffle-grid, and screen-grid). The specimens were cast using separate header and footer beams to distribute the load evenly. Rigid body motion due to uplift was prevented using an external hold-down device. Nominal compressive strength concrete ordered for construction of the wall panels was 2,500 psi (17.2 MPa), but testing revealed an average compressive strength of 5,210 psi (35.9 MPa). Grade 60 reinforcing steel with a tested yield strength of 63 ksi (434.4 MPa) was used. The flat ICF specimen contained three equally spaced #4 dowels to connect the specimen to the footer, three equally spaced #4 vertical reinforcing bars, one #4 horizontal reinforcing bar at the top of the specimen, and two #4 horizontal reinforcing bars at third points along the height. The waffle-grid and screen-grid specimens each contained equally spaced #4 dowels to connect the specimen to the footer, one #4 horizontal reinforcing bar at the top of the specimen, and two #4 horizontal reinforcing bars at approximately third points along the height. No vertical reinforcement was used in the construction of the waffle-grid or screen-grid specimens [13].

The flat ICF specimen experienced initial cracking along the leading edge at the wall panel to footing interface. As the displacement increased, the initial cracking extended to the toe and vertical cracks formed at the bottom of the wall at the leading edge due to bond failure between the concrete and reinforcing dowel. Crushing of the toe was also evident on the compression side. Pullout of the dowel bar from the wall specimen led to gradual decrease in load that was deemed failure of the specimen even though it was restrained against rotation. The peak load was 34,245 lb (152.3 kN).

The waffle-grid ICF specimen experienced cracking along leading edge at the wall panel to footing interface. As the displacement increased, this base crack widened and extended. In addition to the extension of the base cracking, concrete crushing and spalling was observed at the toe. Failure resulted from typical propagation of shear cracks. The peak load was 28,946 lb (128.8 kN).

The screen-grid ICF specimen experienced cracking along leading edge at the wall panel to footing interface. As the displacement increased, an inclined shear crack formed that led to failure of the specimen. The peak load was 27,889 lb (124.1 kN).

## ICF Wall Design for Parallel (In-Plane) Shear

The current design of concrete shear walls for parallel (in-plane) shear follows the provisions outlined in ACI 318 – 99 Section 11.10 [6]. The equations below from Section 11.10 are used to check parallel (in-plane) shear. All vertical cores, both reinforced and unreinforced, are assumed to resist parallel wall shear. Dimensions are often simplified for waffle-grid and screen-grid wall systems that have complex cross sectional geometries. Generally, the web thickness (or effective web thickness) is not considered when evaluating the parallel shear resistance of ICF walls with non-uniform cross sections.

$$V_u \leq \phi V_n$$

$$V_n = V_c + V_s$$

$$V_s = \frac{A_v f_y d}{s_2} \text{ when } V_u > \phi V_c$$

$$d = 0.8l_w$$

$$V_c = 2\sqrt{f'_c}hd$$

where:

$\phi$	Shear strength reduction factor = 0.85 per ACI 9.3.2.
$A_v$	Area of horizontal shear reinforcement within a distance, $s_2$ , and a distance, $d$ , per ACI 11.10 (in <sup>2</sup> ).
$d$	As in above equation per ACI 11.10.4 (in).
$f'_c$	Specified compressive strength of concrete (psi).
$f_y$	Specified yield strength of shear reinforcement (psi).
$h$	Concrete wall thickness (in).
$l_w$	Length of reinforced segment (in).
$s_2$	Spacing of horizontal shear reinforcement (in).
$V_c$	Nominal shear strength of concrete per ACI 11.10.5 (lbs).
$V_n$	Nominal shear strength per ACI 11.2 (lbs).
$V_s$	Nominal shear strength of shear reinforcement per ACI 11.10.9 (lbs).
$V_u$	Factored shear force at section (lbs).

According to ACI-318, a larger value of  $d$ , equal to the distance from the extreme compression fiber to the center of force of all reinforcement in tension, is permitted when determined by strain compatibility analysis.

Where the factored shear force  $V_u$  exceeds shear strength  $\phi V_c$ , horizontal shear reinforcement shall be provided. The ratio of horizontal shear reinforcement area to gross concrete area of the vertical section shall not be less than 0.0025. According to ACI 318, spacing of horizontal reinforcement,  $s_2$ , shall not exceed  $l_w/5$ ,  $3h$ , nor 18 in (457 mm).

Due to the number and size of wall openings in residential construction, particularly on the street facing side of houses, there may be segments with height-to-length aspect ratios greater than or equal to 4:1. In such cases, the behavior of these segments may be dominated by flexural behavior rather than shear behavior. Therefore, the flexural response of such segments in ICF walls should be evaluated using the equations below in accordance with ACI Chapter 10. The amount of tensile reinforcing steel is limited such that it will yield before the concrete reaches its ultimate compressive strength as required by ACI 318 [6].

$$M_u \leq \phi M_n$$

$$\phi M_n \leq \phi A_s f_y \left( d - \frac{a}{2} \right)$$

$$a = \frac{A_s f_y}{0.85 f_c' b}$$

where,

$\phi$	= the strength reduction factor of 0.9 for flexure per ACI 9.3.2
$a$	= depth of equivalent rectangular stress block (in)
$A_s$	= area of tensile reinforcing steel (in <sup>2</sup> )
$b$	= width of compression face of member (in)
$d$	= distance from extreme compression zone (top of beam or toe of wall) to centroid of tensile reinforcement (in)
$f_c'$	= specified compressive strength of concrete (psi)
$f_y$	= specified yield strength of reinforcement (psi)
$M_n$	= nominal moment strength (in-lb)
$M_u$	= moment induced by factored design loads (in-lb)

Regardless of the design conditions, ACI 318 requires a minimum amount of tensile reinforcing steel determined by the greater of the following equations:

$$A_{s,\min} = \frac{3\sqrt{f_c'} b_w d}{f_y} \geq \frac{200 b_w d}{f_y} \quad \text{ACI 318-99 Equation 10-3}$$

In practice, most design applications involve the use of multiple concrete shear wall segments to comprise a building wall line. In residential construction, the configuration and size of these segments (i.e., aspect ratio and wall opening dimensions) can vary significantly. This condition demands the consideration of stiffness of individual wall segments in determining the capacity of a wall line that may be comprised of segments with very different stiffness characteristics. Yet, the current approach favored in residential and low-rise concrete construction determines the

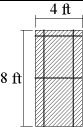
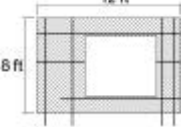
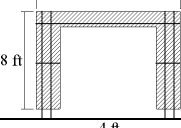
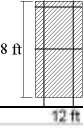
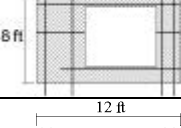
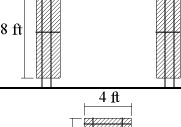
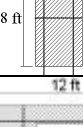
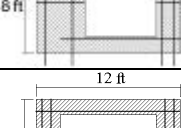
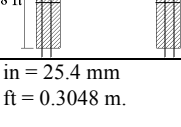
capacity of a concrete (or masonry) shear wall by assuming that all solid portions of a wall, regardless of how far separated or to what degree they are coupled, act as a solid concrete wall of equal length. With this approach, only in cases with extremely scant amounts of solid wall (i.e., more representative of a concrete frame) does flexural capacity control the design solution. This questionable approach is represented in current code documents as well as the general engineering practice [14].

In the *Prescriptive Method* [1], a more conservative approach was used whereby wall bracing amounts in the prescriptive tables were controlled by limiting in-plane flexural capacity of the segments in the wall line in order to determine the required minimum percentage of wall length. An iterative process was used, whereby the length of the flexural elements were varied from 2 ft (0.61 m) to 8 ft (2.4 m) depending on the amount of solid wall length required. The intent of this research was to improve the design method and related assumptions for ICF shear wall design.

## Experimental Program

A total of nine ICF shear walls using three different ICF systems were constructed and tested to evaluate their structural performance using the minimum material and detailing requirements outlined in the *Prescriptive Method* [1]. An overview of the ICF shear wall specimens is given in Table 1. Diagrams showing the shape and dimensions of the individual ICF blocks used to form the shear walls are shown in Figure 1.

**Table 1**  
**Specimen Details**

ICF Specimen	Wall Configuration	Openings	Horizontal Reinforcement	Vertical Reinforcement	Footing/Wall Interface
FLAT No. 1 (Wall 1)		NONE	1 – No. 4 Bar at top 1 – No. 4 Bar at mid-height	1 – No. 4 Bar at each end	2 – No. 4 Bars and No. 4 dowels with 12in embedded in the concrete specimen
FLAT No. 2 (Wall 2)		6ft x 6ft	1 – No. 4 Bar at top 1 – No. 4 Bar at mid-height 1 – No. 4 Bar below opening	1 – No. 4 Bar at each end and at each side of the opening	4 – No. 4 Bars and No. 4 dowels with 12in embedded in the concrete specimen
FLAT No. 3 (Wall 3)		7ft x 8ft	1 – No. 4 Bar at top 1 – No. 4 Bar at mid-height	1 – No. 4 Bar at each end and at each side of the opening	4 – No. 4 Bars and No. 4 dowels with 12in embedded in the concrete specimen
WAFFLE No. 1 (Wall 4)		NONE	1 – No. 4 Bar at top 1 – No. 4 Bar at mid-height	1 – No. 4 Bar at each end	2 – No. 4 Bars and No. 4 dowels with 12in embedded in the concrete specimen
WAFFLE No. 2 (Wall 5)		6ft x 6ft	1 – No. 4 Bar at top 1 – No. 4 Bar at mid-height 1 – No. 4 Bar below opening	1 – No. 4 Bar at each end and at each side of the opening	4 – No. 4 Bars and No. 4 dowels with 12in embedded in the concrete specimen
WAFFLE No. 3 (Wall 6)		7ft x 8ft	1 – No. 4 Bar at top 1 – No. 4 Bar at mid-height	1 – No. 4 Bar at each end and at each side of the opening	4 – No. 4 Bars and No. 4 dowels with 12in embedded in the concrete specimen
SCREEN No. 1 (Wall 7)		NONE	1 – No. 4 Bar at top 1 – No. 4 Bar at mid-height	1 – No. 4 Bar at each end	2 – No. 4 Bars and No. 4 dowels with 12in embedded in the concrete specimen
SCREEN No. 2 (Wall 8)		6ft x 6ft	1 – No. 4 Bar at top 1 – No. 4 Bar at mid-height 1 – No. 4 Bar below opening	1 – No. 4 Bar at each end and at each side of the opening	4 – No. 4 Bars and No. 4 dowels with 12in embedded in the concrete specimen
SCREEN No. 3 (Wall 9)		7ft x 8ft	1 – No. 4 Bar at top 1 – No. 4 Bar at mid-height	1 – No. 4 Bar at each end and at each side of the opening	4 – No. 4 Bars and No. 4 dowels with 12in embedded in the concrete specimen

For SI: 1 in = 25.4 mm  
1 ft = 0.3048 m.

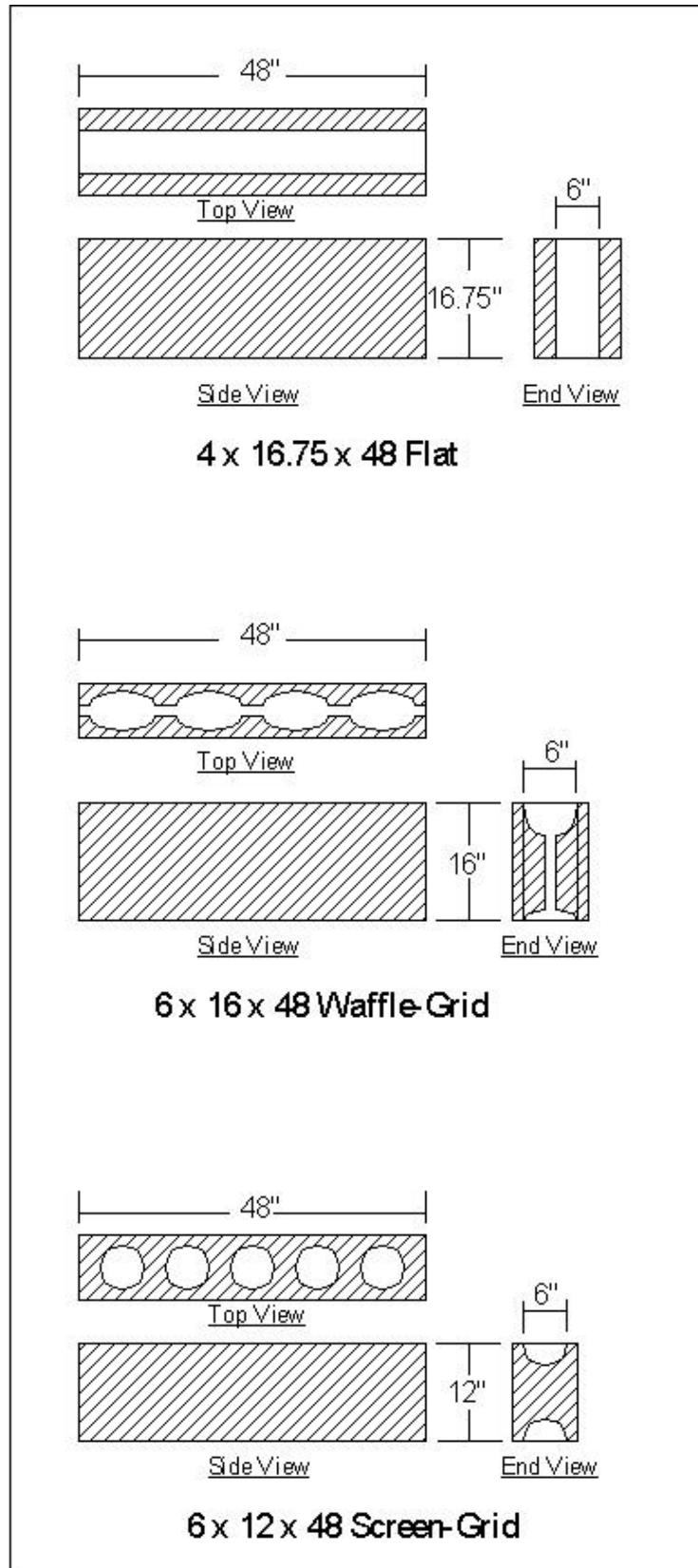


**Figure 1**  
**Diagrams and Dimensions of ICF Systems Used**  
**to Construct the Shear Wall Specimens**

Individual reinforced concrete footers were cast for each of the nine shear walls. Vertical reinforcement, in the form of #4 dowels, was installed in the footing to provide a connection between the footer and shear wall interface. The dowels extended 12 in (305 mm) from the top of the footer into the wall.

Different manufacturers provided the three types of ICFs used to cast the walls on the footer beams. Vertical and horizontal reinforcement was placed in the center of the wall cross section and positions varied as necessary to match the center of the cores in the waffle- and screen-grid ICF systems. Each of the 9 shear walls were cast on individual reinforced concrete footers. The concrete lintels in the waffle-grid and screen-grid shear walls with openings were installed according to the manufacturers' requirements resulting in essentially rectangular beams.

The concrete mix used for all of the footers was specified to provide a minimum 28-day compressive strength of 5,000 psi (34.5 MPa). Quantities of materials incorporated in the selected concrete mix are shown in Table 2. The concrete was supplied by a local ready-mix company and, after certain adjustments were made to optimize workability, had a measured on-site slump of 4 in (102 mm) according to ASTM C143 [15].

The concrete mix used for all of the shear wall test specimens was specified to comply with the *Prescriptive Method* [1]. The mix was designed to provide a minimum 28-day compressive strength of 2,500 psi (17.2 MPa). Quantities of materials specified in the selected concrete mix are shown in Table 2. The concrete was supplied by a local ready-mix company and, after certain adjustments were made to optimize workability (i.e., adding water), had a measured on-site slump of 6 in (152 mm) according to ASTM C143 [15] representing a maximum allowable by the *Prescriptive Method* [1].

**Table 2**  
**Concrete Mix Data**

<b>Reinforced Concrete Footers</b>		<b>ICF Shear Wall Specimens</b>	
<b>Mix Ingredient</b>	<b>Quantity</b>	<b>Mix Ingredient</b>	<b>Quantity</b>
Cement Type I/II	3,760 lb	Cement Type I/II	3,375 lb
Concrete Sand	4,875 lb	Concrete Sand	10,395 lb
#67 Washed Gravel	9,250 lb	#8 Washed Gravel	12,750 lb
Daravair 1000 <sup>1</sup>	30 oz	Daravair 1000 <sup>1</sup>	30 oz
WRDA with HYCOL <sup>2</sup>	115 oz	WRDA with HYCOL <sup>2</sup>	98 oz
Water	170 gal	Water	240 gal

For SI: 1 lb = 4.45 N, 1 oz = 0.28 N, 1 gal = 3.79 l

Notes:

1. Daravair 1000 is an air-entraining admixture and is formulated to comply with Specification for Air-Entraining Admixtures for Concrete, ASTM Designation C 260.
2. WRDA with HYCOL is a water-reducing admixture and is formulated to comply with Specification for Chemical Admixtures for Concrete, ASTM Designation C 194.

Concrete was placed in the ICFs using a concrete pump truck in layers (lifts) of a depth equal to approximately 4 ft (1.22 m). Although a concrete pump truck was used for the pour, a "J"-trap was not utilized on the pipeline, which caused the concrete to free fall from a distance in excess of 20 ft (6.1 m). Each lift was manually consolidated using a 0.5 in (12.7 mm) diameter steel rod. The total time duration of the cast was approximately 5 hours for all specimens because of complications experienced (i.e., blowouts due to excessive drop height of concrete). The complications caused a batch casting time well beyond that recommended. Rainy weather conditions also affected the concrete casting, and the specimens were covered with plastic at the

completion. In total, these conditions may be considered “worst case” representations of residential construction practice and conditions without any special quality control procedures.

Cylindrical concrete specimens were also cast for the footer and shear wall specimens following ASTM C39 [16], ASTM C31 [17], and ASTM C192 [18]. Six 6 in x 12 in (152.4 mm x 304.8 mm) cylinders were cast to represent the concrete incorporated in the footers. After 48 hours the cylinders were split into a moist cured batch and a field cured batch. The cylinders were tested at 28 days to determine the compressive strength of the concrete in the footers. Table 3 summarizes the results.

Fourteen 6 in x 12 in (152.4 mm x 304.8 mm) cylinders were cast to characterize the concrete incorporated in the shear wall specimens. After 48 hours the cylinders were split into two batches. The first batch was moist cured, while the second batch was field cured. The cylinders were tested at 28 and 156 days to determine the standard compressive strength of the concrete and the compressive strength at the time of testing. Table 3 summarizes the results.

**Table 3**  
**Concrete Compression Tests**

<b>Footer Cylinders</b>		<b>Shear Wall Cylinders</b>		
Test Specimens	28 day (psi)	Test Specimens	28 day (psi)	156 day (psi)
Moist-Cured	5,629	Moist-Cured	1,624	1,779
	5,092		1,808	2,046
	5,443		1,931	2,150
<b>AVERAGE</b>	<b>5,388</b>	<b>AVERAGE</b>	<b>1,788</b>	<b>1,992</b>
<b>COV</b>	<b>0.051</b>	<b>COV</b>	<b>0.087</b>	<b>0.096</b>
Field-Cured	4,433	Field-Cured	1,562	1,753
	4,566		1,607	1,794
	4,457		1,599	1,776
<b>AVERAGE</b>	<b>4,486</b>	<b>AVERAGE</b>	<b>1,589</b>	<b>1,774</b>
<b>COV</b>	<b>0.016</b>	<b>COV</b>	<b>0.015</b>	<b>0.012</b>

For SI: 1 psi = 6.90 kPa.

According to ACI 318, the compressive strength,  $f_c$ , should be determined from the moist-cured specimens. However, the field-cured specimens were considered to be more representative of actual conditions. The 28-day compressive strength of the footers was determined to ensure that the footers would not limit failure of the specimens. Moist-cured and field-cured shear wall specimen cylinders were tested at 28 days and at 156 days to determine the concrete compression strength ( $f_c$ ) throughout the test program. An average 28-day value of 1,788 psi (12.3 MPa) was obtained which was 28 percent less than specified. This reduction in strength may be partially attributed to the field conditions experienced at the time of the pour and the maximum slump used. The representative concrete compressive strength of 1,774 psi (12.2 Mpa) was used for the purpose of evaluating the test results relative to ACI 318 predictions.

Grade 60 tensile reinforcing steel was ordered for fabricating the shear wall specimens. Table 4 lists the results of the tension tests performed at the University of Maryland.

**Table 4**  
**Rebar Tension Tests**

Test Specimens	$f_y$ (ksi)
#4 Rebar	
Specimen 1	60.1
Specimen 2	61.8
Specimen 3	60.9
<b>AVERAGE</b>	<b>60.9</b>
<b>COV</b>	<b>0.014</b>

For SI: 1 ksi = 6.90 MPa.

## Test Procedure

Tests on the shear wall specimens commenced at a concrete age of 120 days and continued over a duration of 36 days. The shear walls were tested in a vertical position with overturning restraint and measurements similar to that described in ASTM E72 [20] using monotonic loading. A hydraulic actuator, with a range of 8 in (203.2 mm) and 85,000 lb (378.1 kN) capacity, applied the load to the top of each shear wall through a steel header beam at a rate of 0.2 in/min (Figure 2). The steel load beam was attached to the specimens using 3/4 in (19.1 mm) bolts 1 ft (0.3 m) on center that were embedded in the specimens at the time of the pour. An external hold-down was provided on the leading edge of the shear walls to prevent an overturning failure mode. The restraint did allow the specimens to rotate a small amount, but prevented an overturning failure from dominating the behavior of the specimens. A 100,000 lb (444.8 kN) load cell was attached to the end of the actuator to enable load recordings. The load cell calibration was verified using the NAHB Research Center's Universal Test Machine (NIST Traceable).

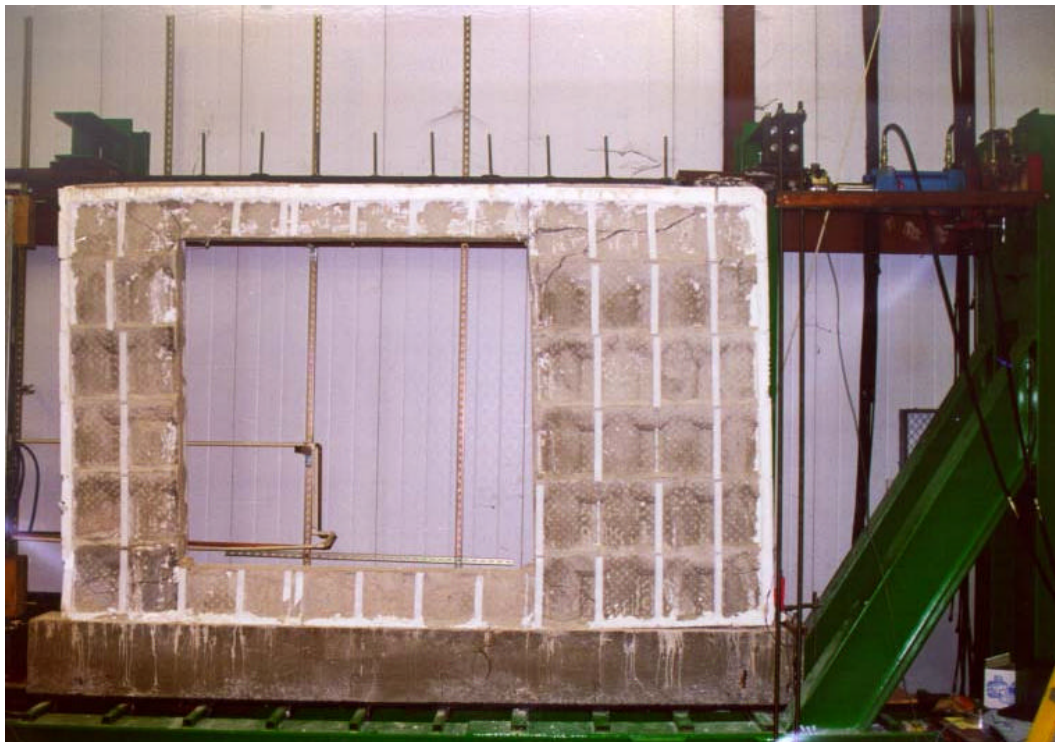


**Figure 2**  
**NAHB Research Center's Shear Wall Testing Facility**

Three linear variable differential transformers (LVDT) were used to measure the displacement of the specimens during the tests. The LVDTs measured the horizontal displacement of the top of the wall, the horizontal displacement (or slip) of the bottom of the specimen, and uplift at the leading edge relative to the footing beam. Two dial gauges were used to independently measure the horizontal slip and uplift of the footing beam.

All tests were one directional, displacing the top of the wall to a maximum of 4 in (101.6 mm) over a twenty minute period. Data from the load cells and LVDTs were collected 2 times per second. Data from the dial gauges were manually recorded at 500 lb (2.24 kN) increments up to 5,000 lb (22.2 kN) and at 1,000 lb (4.45 kN) increments thereafter. Each of the nine wall configurations was tested once. Items of interest were observations of cracking during displacement history, ultimate load capacity, load distribution, initial stiffness, and energy dissipated. Load-displacement curves were plotted for each of the wall specimens to better understand and compare the behavior of the walls.

## Test Results and Discussion

### *General Observations of Wall Behavior*

Qualitative observations of the performance of the ICF shear wall specimens were noted during the tests. The observations were mostly visual such as crack formation, growth, and propagation. The formation and growth of cracks on the ICF panels detail the basic mechanisms of response to the monotonic drift history. A summary of the important events in each shear wall test is given in Tables 5 through Table 7. Figures 3 through 13 illustrate the observed behavior.

**Table 5  
Test Observations for the Flat Shear Wall Specimens**

<b>Flat No. 1 (Wall 1) – 4ft x 8ft</b>		
<b>Lateral Load (lbs)</b>	<b>Lateral Displacement (in)</b>	<b>Comments</b>
18,000	1.100	Crushing of concrete at the top of the specimen near the hold-down restraint and load application due to uplift at leading edge.
18,600	1.130	Uplift at leading edge. Failure at concrete reinforcing dowel interface.
20,800	1.770	Crushing and spalling increasing at leading edge.
<b>Flat No. 2 (Wall 2) – 12ft x 8ft with Window Opening</b>		
<b>Lateral Load (lbs)</b>	<b>Lateral Displacement (in)</b>	<b>Comments</b>
4,100	0.190	Hairline cracks forming around corners of window (Figure 3).
7,500	0.330	Visible uplift of 4ft panel. No uplift of 2ft panel.
15,150	0.590	Crack at the top corner of the specimen where the load is applied to the top right corner of the window opening widens to 1/4 in.
38,500	1.250	Crack at the top corner of the specimen where the load is applied to the top right corner of the window opening widens to 7/8 in (Figure 4). Distress in 2ft segment only near opening corners.
<b>Flat No. 3 (Wall 3) – 12ft x 8ft with Garage Opening</b>		
<b>Lateral Load (lbs)</b>	<b>Lateral Displacement (in)</b>	<b>Comments</b>
1,610	0.530	Cracking along the uplift edges of both panels.
1,760	0.760	Cracks near the corners of the garage opening.
2,010	1.070	Propagation and widening of cracks from the loading corner to the top corner of the opening (Figure 5). Additional cracking on trailing wall segment around garage opening.
1,620	2.510	Test terminated. Noticeable racking of specimen. Apparent rotation of both wall segments (Figure 6).



**Figure 3**  
Typical Hairline Cracking at the Corners of the Window Opening

Failure Crack



**Figure 4**  
Failure Mechanism of Flat No. 2 Wall Specimen



**Figure 5**  
**Failure Mechanism of Flat No. 3 Wall Specimen**



**Figure 6**  
**Final Lateral Displacement of Flat No. 3 Wall Specimen**

**Table 6**  
**Test Observations for the Waffle-Grid Shear Wall Specimens**

<b>Waffle-Grid No. 1 (Wall 4) – 4ft x 8ft</b>		
<b>Lateral Load (lbs)</b>	<b>Lateral Displacement (in)</b>	<b>Comments</b>
8,400	0.620	Uplift at leading edge. Failure at concrete reinforcing dowel interface.
10,000	0.850	Crushing of concrete at the top of the specimen near the hold-down restraint and load application.
17,000	1.200	Hairline crack forming at 45-degrees at the top corner of the specimen where the load is applied.
17,800	1.260	Hairline crack widens and propagates to cause failure (Figure 7).
<b>Waffle-Grid No. 2 (Wall 5) – 12ft x 8ft with Window Opening</b>		
<b>Lateral Load (lbs)</b>	<b>Lateral Displacement (in)</b>	<b>Comments</b>
7,100	0.330	Visible uplift of 4ft panel. No uplift of 2ft panel.
12,500	0.540	Cracking from loaded corner to adjacent window corner.
15,500	1.150	Cracking from loaded corner to adjacent window corner widening to 3/8 in.
17,000	1.270	Cracking around the corners of the window opening (Figure 8).
17,500	1.320	Crushing of concrete at the top of the specimen near the hold-down restraint and load application. Uplift at leading edge.
18,100	1.400	Cracking from loaded corner to adjacent window corner widening to 3/4 in (Figure 9). Distress in 2ft segment only near opening corners.
<b>Waffle-Grid No. 3 (Wall 6) – 12ft x 8ft with Garage Opening</b>		
<b>Lateral Load (lbs)</b>	<b>Lateral Displacement (in)</b>	<b>Comments</b>
800	0.160	Cracking along the uplift edges of both panels.
1,000	0.220	Crack near the corner of the garage opening.
1,500	0.340	Crushing at the toe of both 2ft panels
2,000	0.600	Widening of crack from loading corner to the top corner of the opening
1,330	0.990	Test terminated. Noticeable racking of specimen. Apparent lateral load distribution to both wall segments. Severe cracking around corner of garage opening (Figure 10).



**Figure 7**  
**Failure Mechanism of Waffle No. 1 Wall Specimen**



**Figure 8**  
**Typical Hairline Cracking at the Corner of the Window Opening (Waffle No. 2)**



**Figure 9**  
**Failure Mechanism of Waffle No. 2 Wall Specimen**

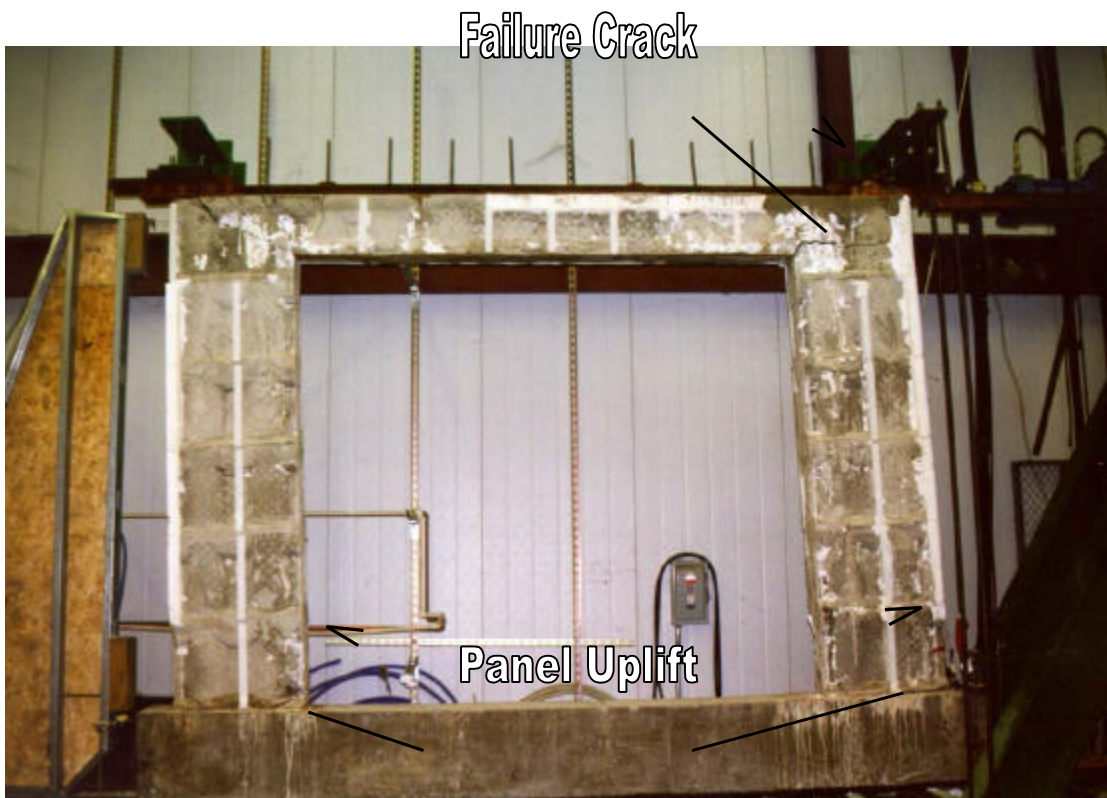


**Figure 10**  
**Final Lateral Displacement of Waffle No. 3 Wall Specimen**

**Table 7**  
**Test Observations for the Screen-Grid Shear Wall Specimens**

<b>Screen-Grid No. 1 (Wall 7) – 4ft x 8ft</b>		
<b>Lateral Load (lbs)</b>	<b>Lateral Displacement (in)</b>	<b>Comments</b>
11,400	0.860	Uplift and cracking at leading edge. Crushing at hold-down
13,000	1.130	Hairline cracks forming from loading corner across specimen at approximately 20-degrees.
16,500	1.550	Crushing of concrete at the top of the specimen near the hold-down restraint and load application.
17,200	1.700	Widening and propagation of cracks from loading corner caused failure (Figure 11).
<b>Screen-Grid No. 2 (Wall 8) – 12ft x 8ft with Window Opening</b>		
<b>Lateral Load (lbs)</b>	<b>Lateral Displacement (in)</b>	<b>Comments</b>
2,700	0.160	Initial crack formed at mid-height on the leading edge to the bottom corner of the window opening.
5,200	0.550	Cracking around the corners of the window opening. A hairline crack formed at 45-degrees at the top corner of the specimen where the load is applied.
5,600	0.740	45-degree crack widened and additional cracks formed around this crack (Figure 12).
<b>Screen-Grid No. 3 (Wall 9) – 12ft x 8ft with Garage Opening</b>		
<b>Lateral Load (lbs)</b>	<b>Lateral Displacement (in)</b>	<b>Comments</b>
1,100	0.120	Cracking along the uplift edges of both panels.
1,990	0.700	Cracks near corners of garage opening.
1,750	0.850	Crushing at the toe of both 2ft panels
1,660	0.940	Widening of crack from loading corner to the top corner of the garage opening. Spalling of concrete at leading reinforcing dowel.
1,580	1.110	Test terminated. Noticeable racking of specimen. Apparent rotation of both wall segments. Severe cracking around corner of garage opening (Figure 13).

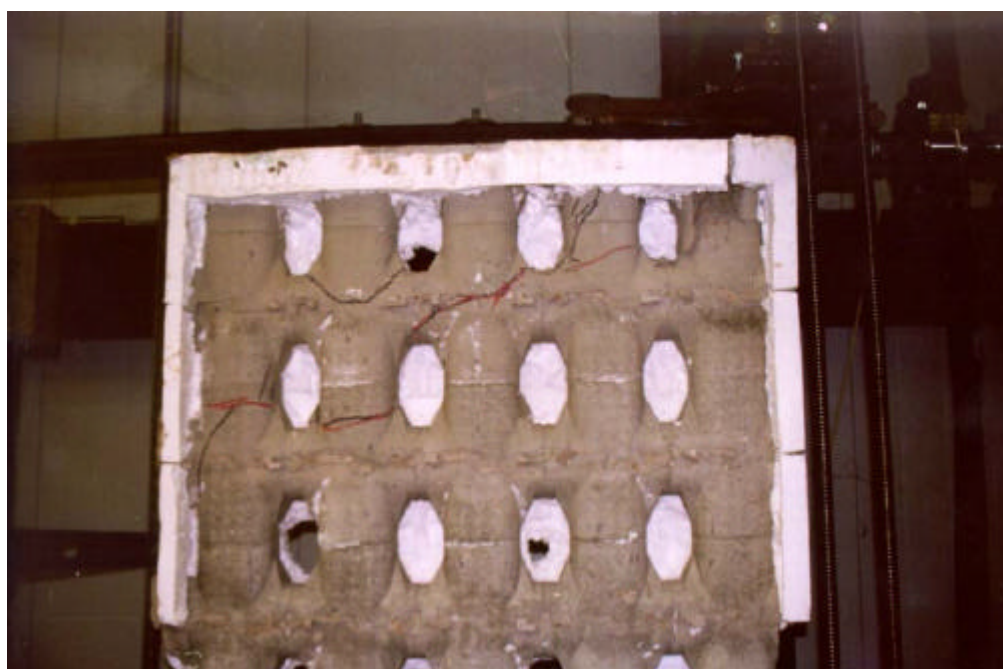


**Figure 11**  
**Failure Mechanism of Screen No. 1 Wall Specimen**

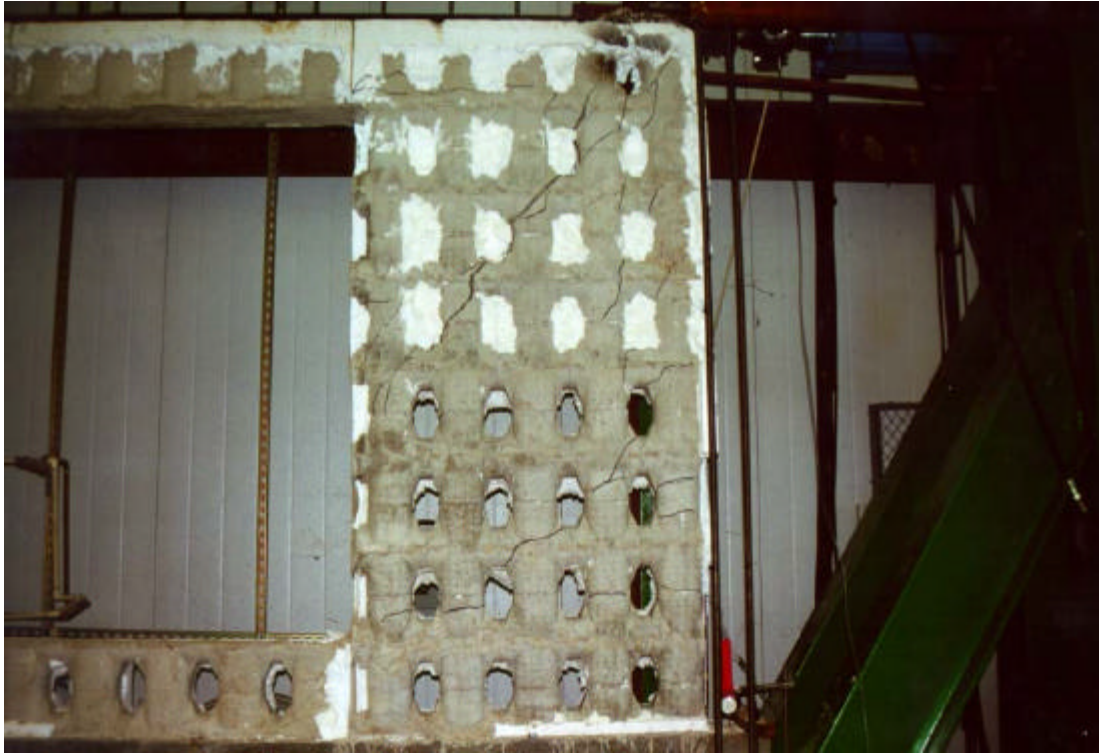


**Figure 12**  
**Failure Mechanism of Screen No. 2 Wall Specimen**

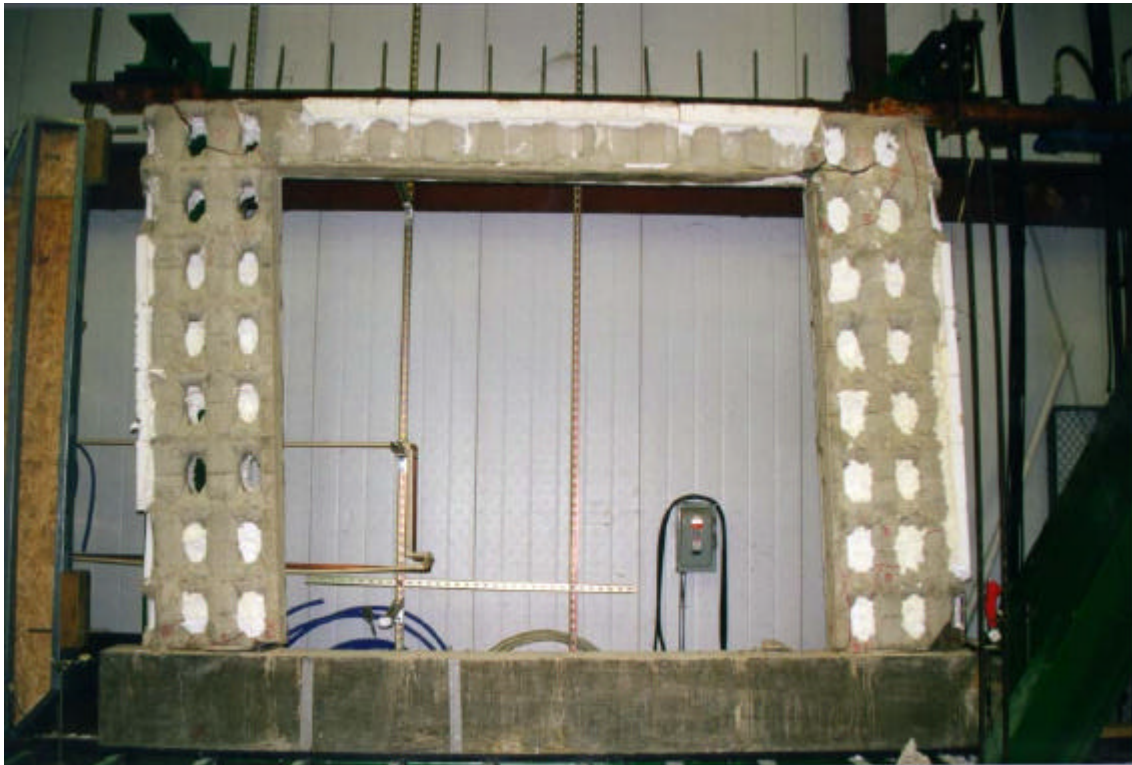


**Figure 13**  
**Final Lateral Displacement of Screen No. 3 Wall Specimen**

With only one exception, each of the three shear wall configurations tested behaved similarly with a typical shear controlled failure mode regardless of the ICF system used. The one exception – the flat 4 ft x 8 ft (1.22 m x 2.44 m) specimen – never experienced shear cracks, but rather failed due to crushing and spalling of the concrete at the hold-down restraint and load application corner.

*Force-Displacement Response*

The responses of the shear wall specimens to the displacement history are shown in the force-displacement curves of Figures 14 through 19. The force-displacement curves demonstrate that the response of the shear wall specimens was essentially linear during the initial loading and became non-linear as the displacement increased. In most cases, the behavior of the walls resembles an elastic-plastic system with a well defined proportional limit. This proportional limit corresponds to either the formation of shear cracks or the initial overturning failure outlined in Tables 5 through 7.

The ultimate shear load,  $F_{max}$ , as well as the corresponding displacement,  $\Delta_{Fmax}$ , was gathered directly from the data. Failure was determined as the capacity of the specimen immediately prior to a significant decrease in strength or when the load dropped to  $0.8F_{max}$ , whichever occurred first. These loads and displacements are presented in Table 8. It is not clear why Screen No. 2 experienced an unusually low ultimate load compared to the other specimens.

**Table 8**  
**Force-Displacement Data Summary from Testing**

	Wall Specimens								
	1	2	3	4	5	6	7	8	9
	Flat No. 1	Flat No. 2	Flat No. 3	Waffle No. 1	Waffle No. 2	Waffle No. 3	Screen No. 1	Screen No. 2	Screen No. 3
$F_{max}$ (kips)	20.84	38.57	2.02	17.77	18.11	2.03	17.69	5.63	2.00
$\Delta_{Fmax}$ (in)	1.79	1.25	1.07	1.17	1.40	0.66	1.72	0.77	0.70
$F_{failure}$ (kips)	18.8	30.9	1.6	12.9	14.4	1.3	14.1	3.9	1.6
$\Delta_{failure}$ (in)	2.24	1.95	2.52	1.25	2.44	0.99	2.02	1.04	1.12
Initial Stiffness (kips/in)	12.6	24.2	16.8	12.8	21.6	15.2	13.7	19.6	12.9
Energy Dissipated (kips-in)	31.4	44.6	4.2	10.72	31.61	1.50	22.1	5.3	1.7

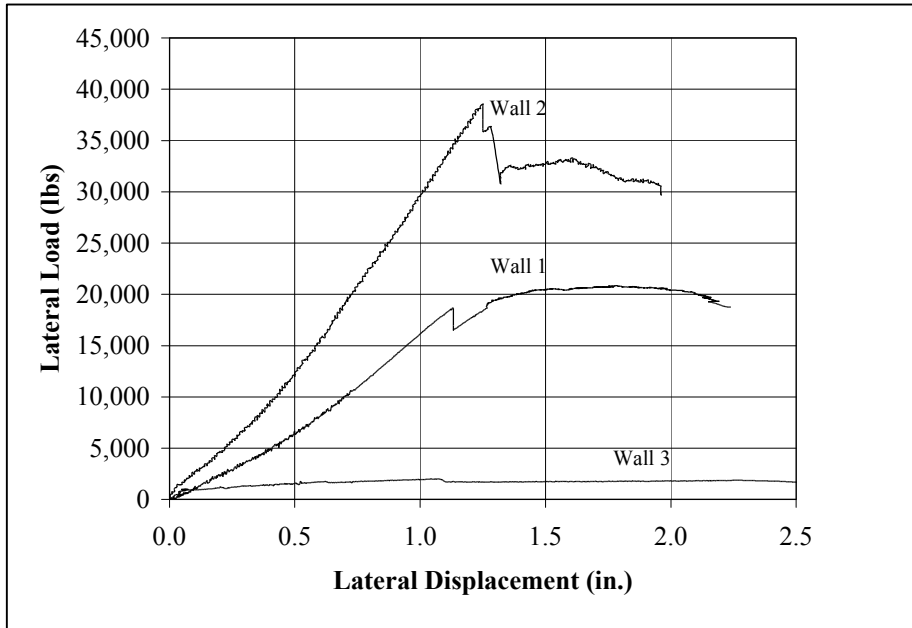


**Figure 14**  
**Force-Displacement Response for the Flat ICF Shear Wall Specimens**  
**(Wall 1, Wall 2, and Wall 3)**

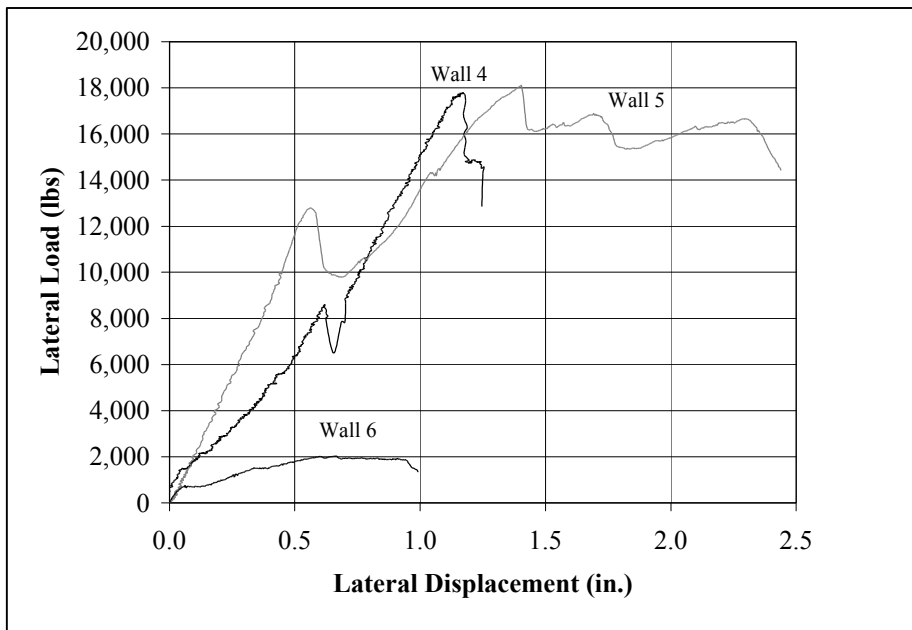


**Figure 15**  
**Force-Displacement Response for the Waffle-Grid ICF Shear Wall Specimens**  
**(Wall 4, Wall 5, and Wall 6)**

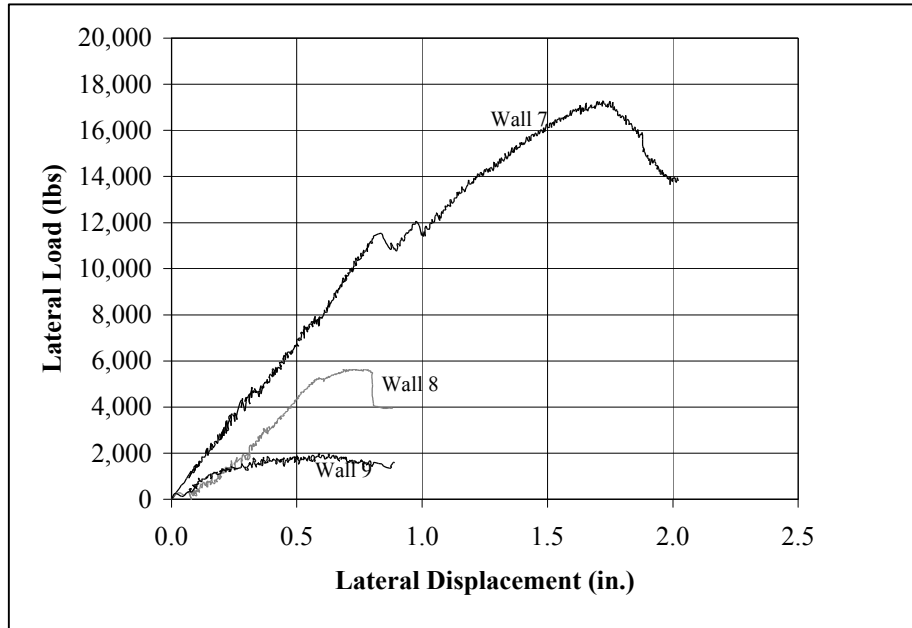


**Figure 16**  
**Force-Displacement Response for the Screen-Grid ICF Shear Wall Specimens (Wall 7, Wall 8, and Wall 9)**

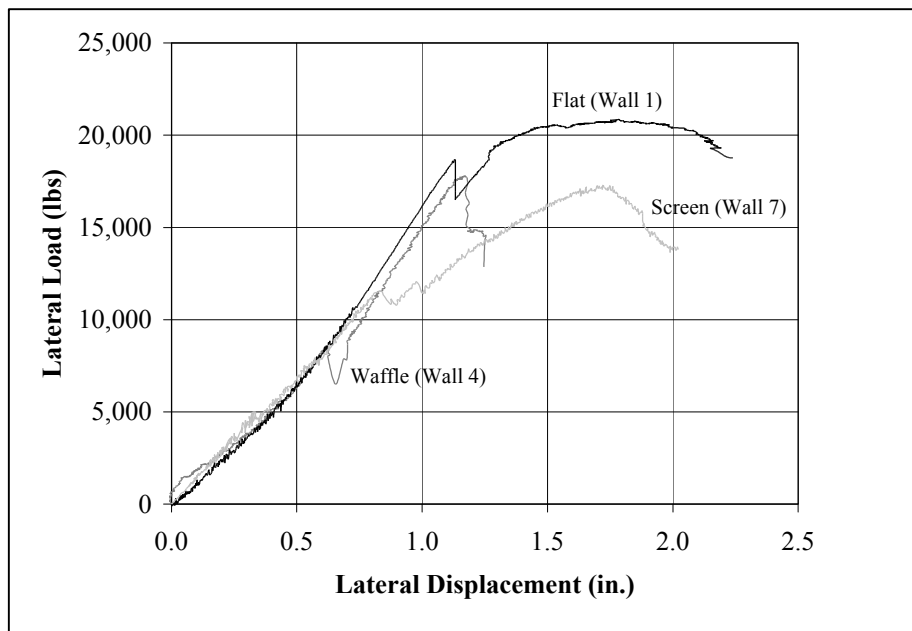


**Figure 17**  
**Force-Displacement Response for the 4ft x 8ft ICF Shear Wall Specimens (Wall 1, Wall 4, and Wall 7)**

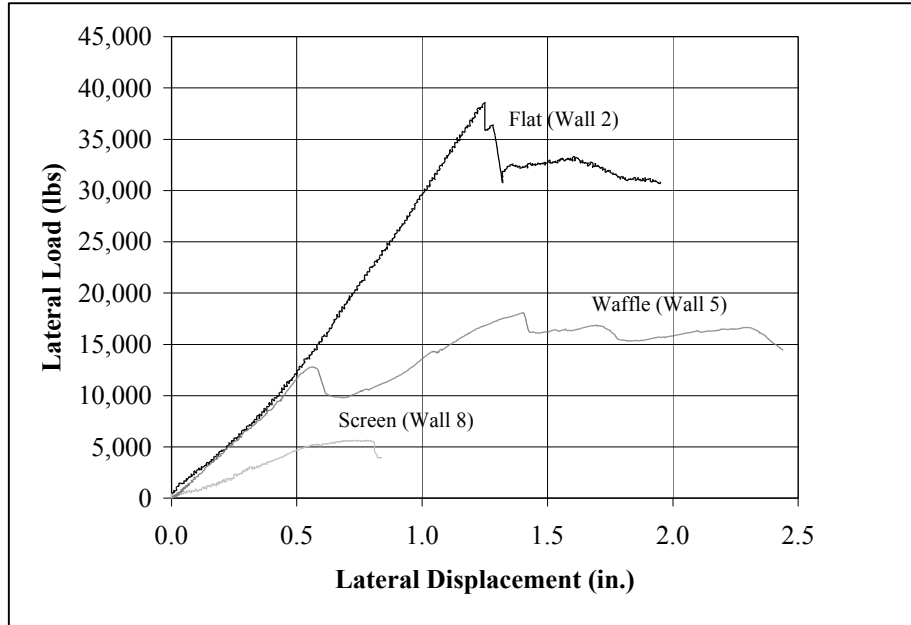


**Figure 18**  
**Force-Displacement Response for the 12ft x 8ft with Window Opening ICF Shear Wall Specimens (Wall 2, Wall 5, and Wall 8)**

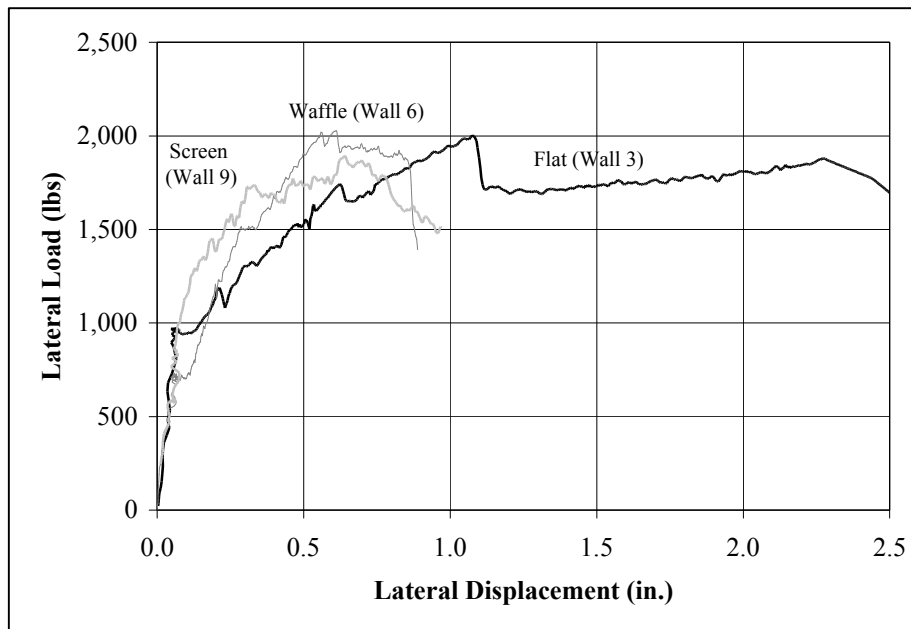


**Figure 19**  
**Force-Displacement Response for the 12ft x 8ft with Garage Opening ICF Shear Wall Specimens (Wall 3, Wall 6, and Wall 9)**

### Initial Stiffness

The initial portion of the force-displacement curves were fit with a linear least-squares trend, the slope of which is taken as the initial stiffness ( $K$ ). That portion of the curve for which the magnitude of the force did not exceed 40-percent of the peak load was used in the calculation. The linear least-squares trend provided a very good fit to the data. The initial stiffnesses are listed in Table 8.

In general, the initial stiffnesses for the 4 ft x 8 ft (1.22 m x 2.44 m) panels were all within 8-percent regardless of ICF system used. This may be explained by the fact that overturning rather than shear cracking controlled the initial behavior of the specimens. For the 12 ft x 8 ft (3.66 m x 2.44 m) specimens, the flat ICF had approximately a 10-percent and 20-percent higher initial stiffness than the waffle-grid and screen-grid, respectively, regardless of opening size.

The load distribution between the 4 ft (1.22 m) and 2 ft (0.61 m) full-height wall segments (i.e., the specimens with the window opening) was investigated using the stiffness from the test data. An effective stiffness was calculated for specimens containing the window opening using the stiffnesses determined in Table 8. The specimen was simplified into two springs in parallel. Since the system is considered a parallel spring system, both full height wall segments (or “springs”) realize equal displacements. Hence the effective stiffness ( $K_{effective}$ ) for the window specimen is defined as

$$K_{effective} = K_{4ft} + K_{garage}/2$$

$K_{4ft}$  is the tested stiffness of the 4 ft (1.2 m) wall specimens and  $K_{Garage}/2$  is the stiffness of the 2 ft (0.61 m) wall segment (as determined by taking one-half of the tested stiffness of the garage opening specimens which had two 2ft (0.61 m) segments). Table 9 summarizes the calculations. This method provides very reliable results for determining the stiffness of specimens with dissimilar full height wall segments when the stiffnesses of the individual segments are known. This suggests that the nominally reinforced lintels used in the specimens initially provided adequate transfer of the load to the trailing 2 ft (0.61 m) wall segment.

**Table 9**  
**Comparison of Actual to Effective Stiffness**

ICF TYPE	Tested Stiffnesses (kip/in)			$K_{effective}$ (kip/in)	Ratio
	$K_{4ft}$	$K_{Garage}$	$K_{Window}$		
FLAT	12.6	16.8	24.2	21.00	1.15
WAFFLE	12.8	15.2	21.6	20.40	1.06
SCREEN	13.7	12.9	19.6	20.15	0.97

### Energy Dissipated

The toughness of a wall can be quantified by its ability to dissipate energy while deforming. Cumulative energy dissipation was obtained by integrating the force-displacement curves to determine the area under each up to a significant decrease in resistance or  $0.8F_{max}$ . These values are listed in Table 8.

The flat ICF shear walls were able to maintain near peak loads for larger displacements than were the waffle-grid and screen-grid specimens. This resulted in larger energy dissipation values. However, there was no obvious distinction in energy dissipation performance between the waffle-

grid and screen-grid specimens. Waffle No. 1 experienced an abrupt shear failure, and this resulted in the comparatively low calculated value of energy dissipation (low ductility). The low ultimate load experienced by Screen No. 2 adversely affected the energy dissipation calculations for this specimen.

## Design Evaluation

In this section, current design methods for ICF shear walls are compared to the test results from the previous section. A previous research program evaluated the effectiveness of concrete lintels without shear reinforcement and produced more efficient lintel designs for ICF construction [21]. It was determined that an effective web thickness of 3.2 in (81.3 mm) and 2.0 in (50.8 mm) provided accurate predictions of the shear capacity of the waffle-grid and screen-grid lintels tested, respectively. In this study of shear walls, current design methodologies and the effective web thickness approach are evaluated. Effective widths for shear walls are expected to differ from those developed from the lintel research since the shear loads are applied in a horizontal direction compared to a vertical direction for lintels. For the waffle-grid and screen-grid specimens, the cross-sectional areas of concrete differ in the horizontal and vertical planes.

### *Flat Specimens*

Two prediction models were investigated for the flat specimens. Model 1 assumes all full height wall segments 2 ft (0.61 m) or greater in length act together as a continuous solid wall to resist a concentrated lateral force at the top of the wall. Model 2 assumes 2 ft (0.61 m) solid wall segments will be dominated by flexural behavior while 4 ft (1.22 m) solid wall segments will be dominated by shear failure. Table 10 summarizes the predictions of Model 1 and Model 2. Appendix A includes the calculations used to develop Table 10.

**Table 10**  
**Tested vs. Predicted Shear Capacities for Flat Test Specimens using Model 1 and Model 2**

Test Specimen	Failure Mode <sup>1</sup>	Tested Shear Capacity (lbs)	Model 1		Model 2	
			Predicted Shear Capacity (lbs)	Ratio Tested/Predicted	Predicted Shear Capacity (lbs)	Ratio Tested/Predicted
Flat No. 1	C	20,840	24,018	0.87	24,018	0.87
Flat No. 2	S	38,570	34,389	1.12	26,375	1.46
Flat No. 3	B	2,020	21,357	0.09	5,176	0.39

For SI: 1 ft = 0.30 m; 1 in = 25.4 mm; 1 lb = 4.45 N, 1 in-lb = 0.113 N-m

Notes:

1. Failure Modes are as follows:

- B: Combination of bending and overturning failure without a distinct shear failure.
- C: Crushing of concrete at load application and external hold-down restraint with no shear cracking.
- S: Shear before yield of tensile steel.

Since the failure mode for Flat No. 1 specimen was characterized by crushing of the concrete at the hold-down restraint as a result of the test configuration, it is difficult to determine the validity of the prediction models for this specimen. Prediction Model 1 and Model 2 provide a conservative estimate of the shear capacity for Flat No. 2. Model 1 provides a very non-conservative estimate of the shear capacity of Flat No. 3 specimen. Although to a lesser degree, Model 2 also provides a non-conservative estimate for Flat No.3.

## Waffle – Grid Specimens

Two prediction models were investigated for the waffle-grid specimens. Model 1 assumes all solid wall segments 2 ft (0.61 m) or greater in length act as a continuous solid wall to resist a concentrated lateral force at the top of the wall. Model 2 assumes that 2 ft (0.61 m) solid wall segments will be dominated by flexural behavior and that 4 ft (1.22 m) solid wall segments will be dominated by shear failure. Model 1 and Model 2 only consider the area of the vertical cores in determining the shear capacity of the specimens. Table 11 summarizes the predictions by the two models. Appendix A includes the calculations used to develop Table 11.

**Table 11**  
**Tested vs. Predicted Shear Capacities for Waffle-Grid Specimens using Model 1 and Model 2**

Test Specimen	Failure Mode <sup>1</sup>	Tested Shear Capacity (lbs)	Model 1		Model 2	
			Predicted Shear Capacity (lbs)	Ratio Tested/Predicted	Predicted Shear Capacity (lbs)	Ratio Tested/Predicted
Waffle No. 1	S	17,770	9,949	1.79	9,949	1.79
Waffle No. 2	S	18,110	14,213	1.27	12,511	1.45
Waffle No. 3	B	2,030	8,527	0.24	5,089	0.40

For SI: 1 ft = 0.30 m; 1 in = 25.4 mm; 1 lb = 4.45 N, 1 in-lb = 0.113 N-m

Notes:

1. Failure Modes are as follows:

- B: Combination of bending and overturning failure without a distinct shear failure.
- C: Crushing of concrete at load application and external hold-down restraint with no shear cracking.
- S: Shear before yield of tensile steel.

Prediction Model 1 and Model 2 provide conservative estimates of the shear capacity for Waffle No. 1 and Waffle No. 2. Model 1 provides a very non-conservative estimate of the shear capacity of Waffle No. 3 specimen. Although to a lesser degree, Model 2 also provides a non-conservative estimate for Waffle No. 3.

Model 2 was used to determine an effective web thickness for the 6 in (152 mm) waffle-grid shear walls. The effective thickness is determined by setting the shear prediction equation (Model 2) equal to the tested shear capacity. Resistance factors are not applied since the comparison is based on ultimate test values. Table 12 summarizes the effective thicknesses developed using Model 2. Appendix A includes the calculations used to develop Table 12.

**Table 12**  
**Effective Wall Thickness for 6 in Waffle-Grid Specimens**

Test Specimen	Failure Mode	Tested Shear Capacity (lbs)	Effective Web Thickness (in)
Waffle No. 1	S	17,770	4.46
Waffle No. 2	S	18,110	3.99
Waffle No. 3	B	2,030	- <sup>1</sup>

For SI: 1 ft = 0.30 m; 1 in = 25.4 mm; 1 lb = 4.45 N

Notes:

- 1. Bending and overturning governs design, therefore effective web thickness for shear calculations is not applicable

## Screen – Grid Specimens

Two prediction models were investigated for the screen-grid specimens. Model 1 assumes all solid wall segments 2 ft (0.61 m) or greater in length act as a continuous solid wall to resist a concentrated lateral force at the top of the wall. Model 2 assumes that 2 ft (0.61 m) solid wall segments will be dominated by flexural behavior and that 4 ft (1.22 m) solid wall segments will be dominated by shear failure. Model 1 and Model 2 only consider the area of the vertical cores in determining the shear capacity of the specimens. Table 13 summarizes the predictions by the three models. Appendix A includes the calculations used to develop Table 13.

**Table 13**  
**Tested vs. Predicted Shear Capacities for Screen-Grid Specimens using Model 1 and Model 2**

Test Specimen	Failure Mode <sup>1</sup>	Tested Shear Capacity (lbs)	Model 1		Model 2	
			Predicted Shear Capacity (lbs)	Ratio Tested/Predicted	Predicted Shear Capacity (lbs)	Ratio Tested/Predicted
Screen No. 1	S	17,690	10,235	1.73	10,235	1.73
Screen No. 2	S	5,630	14,784	0.38	13,139	0.43
Screen No. 3	B	2,000	9,098	0.22	5,807	0.34

For SI: 1 ft = 0.30 m; 1 in = 25.4 mm; 1 lb = 4.45 N, 1 in-lb = 0.113 N-m

Notes:

1. Failure Modes are as follows:

- B: Combination of bending and overturning failure without a distinct shear failure.
- C: Crushing of concrete at load application and external hold-down restraint with no shear cracking.
- S: Shear before yield of tensile steel.

Both of the prediction models provided conservative estimates of the shear capacity for Screen No. 1. The Screen No. 2 wall specimen failed prematurely, therefore it is difficult to determine which model provides the best shear capacity prediction though Model 2 provided the least error. Model 1 provides a non-conservative estimate of the shear capacity of Screen No. 3 specimen. Although to a lesser degree, Model 2 also provides a non-conservative estimate for Screen No. 3.

Model 2 was used to determine an effective wall thickness for the 6 in (152 mm) screen-grid shear walls. The effective thickness is determined by setting the shear prediction equation (Model 2) equal to the tested shear capacity. Table 14 summarizes the effective thicknesses developed using Model 2. The effective web thickness of 0.82 in (20.8 mm) determined for Screen No. 2 is not considered reliable since the specimen failed prematurely. Appendix A includes the calculations used to develop Table 14.

**Table 14**  
**Effective Wall Thickness for 6 in Screen-Grid Specimens**

Test Specimen	Failure Mode	Tested Shear Capacity (lbs)	Effective Web Thickness (in)
Screen No. 1	S	17,690	4.42
Screen No. 2	S	5,630	0.82
Screen No. 3	S	2,000	- <sup>1</sup>

For SI: 1 ft = 0.30 m; 1 in = 25.4 mm; 1 lb = 4.45 N

Notes:

- 1. Bending and overturning governs design, therefore effective web thickness for shear calculations is not applicable

The above analysis suggests that Model 1 and Model 2 provide conservative estimates for specimens containing wall segments with a 2:1 aspect ratio. This excludes the anomalous test specimen Screen No. 2. Neither Model 1 nor Model 2 accurately predicts the behavior of the specimens containing the garage door. This may be due to the specimen's tendency to overturn as a result of the narrow wall segments or due to an inefficient load transfer through the lintel from the leading pier to the trailing pier near ultimate load. A final reason may be due to the stress concentrations that formed around the corners of the openings, which led to premature reductions in load and stiffness before a traditional shear or flexural failure. It is unclear how specimens with smaller openings or larger lintels would have preformed under the same loading. It should be noted that the typical design practice of Model 1 is a less conservative estimate than Model 2 for the walls tested in this study (i.e., walls containing narrow segments with aspect ratios greater than 2:1 and without any special reinforcement detailing). However, both methods provide generally conservative estimates of actual wall performance when the walls contain large openings and narrow wall segments.

Effective wall thicknesses were developed for the waffle- and screen-grid specimens in Table 12 and Table 14. The procedure followed the methods used to develop the effective web thicknesses developed in the report entitled *Testing and Design of Lintels Using Insulating Concrete Forms* [21]. Due to the size of the test matrix and the anomalous data point in Screen No. 2, the effective wall thicknesses put forth in this report should be considered preliminary. Table 15 indicates that the data published by the Portland Cement Association (PCA) in the report entitled *In-Plane Lateral Load Resistance of Wall Panels in Residential Buildings* [13], produce similar effective wall thicknesses for the 6 in (152.4 mm) waffle- and screen-grid specimens.

**Table 15**  
**Effective Wall Thickness from Data Published by PCA**

Test Specimen	Tested Shear Capacity (lbs)	Concrete Compressive Strength (psi)	Effective Web Thickness <sup>1</sup> (in)
4ft x 8ft Waffle-Grid (6 in)	28,946	5,210	4.56
4ft x 8ft Screen-Grid (6 in)	27,889	5,210	4.39

For SI: 1 ft = 0.30 m; 1 in = 25.4 mm; 1 lb = 4.45 N

Notes:

1. Developed from the equation  $V_c = 2\sqrt{f'_c}b_wd$  where  $d = 48\text{in} - 4\text{in} = 44\text{in}$ .

## Investigation of an Empirical Design Method

Recent testing of wood-framed and steel-framed shear walls that exhibit diaphragm (plate) action have shown that the effect of openings in wall lines of various configurations can be accurately predicted using a rather simple empirically derived relationship [22 – 29]. The method, known as the Perforated Shear Wall Method, relates the opening area ratio ( $r$ ) and unit shear capacity to the overall wall shear capacity. The opening area ratio is determined as follows:

$$r = \frac{1}{1 + \frac{A_o}{HSL_i}}$$

where:

- $A_o$  = total area of openings
- $H$  = height of the wall
- $L_i$  = length of full height wall segment

The overall wall shear capacity is determined as follows:

$$F = F_{unit} \times L_{wall} \times \left[ \frac{r}{3-2r} \text{ or } \frac{r}{2-r} \right]$$

where:

- $F$  = wall shear capacity (lbs)
- $F_{unit}$  = unit shear capacity of wall system usually based on 4 ft to 8 ft long wall segments (2:1 or 1:1 height-to-length aspect ratio)
- $L_{wall}$  = total length of wall including openings
- [ ] = formula in brackets is an empirical relationship based on test data

Figure 20 graphically displays the relation between the opening area ratio and the ultimate lateral load for each of the walls tested. The ultimate lateral load for a 12 ft x 8 ft (3.66 m x 2.44 m) wall without openings was determined by multiplying the tested unit shear for the 4 ft x 8 ft (1.22 m x 2.44 m) wall specimen by the wall length of 12 ft (3.66 m). This calculation is done to compare the specimens with openings to a wall of the same length with no openings. The estimate is considered conservative since the overturning forces would be reduced for the longer specimen. The estimated shear failure for the flat specimen without an opening was used in lieu of the tested value since this specimen never experienced a traditional shear failure but rather a compression failure at the hold-down restraint. In this case, the ultimate estimated shear value for the 4 ft x 8ft (1.22 m x 2.44 m) was determined using the ACI equations outlined previously in this report.

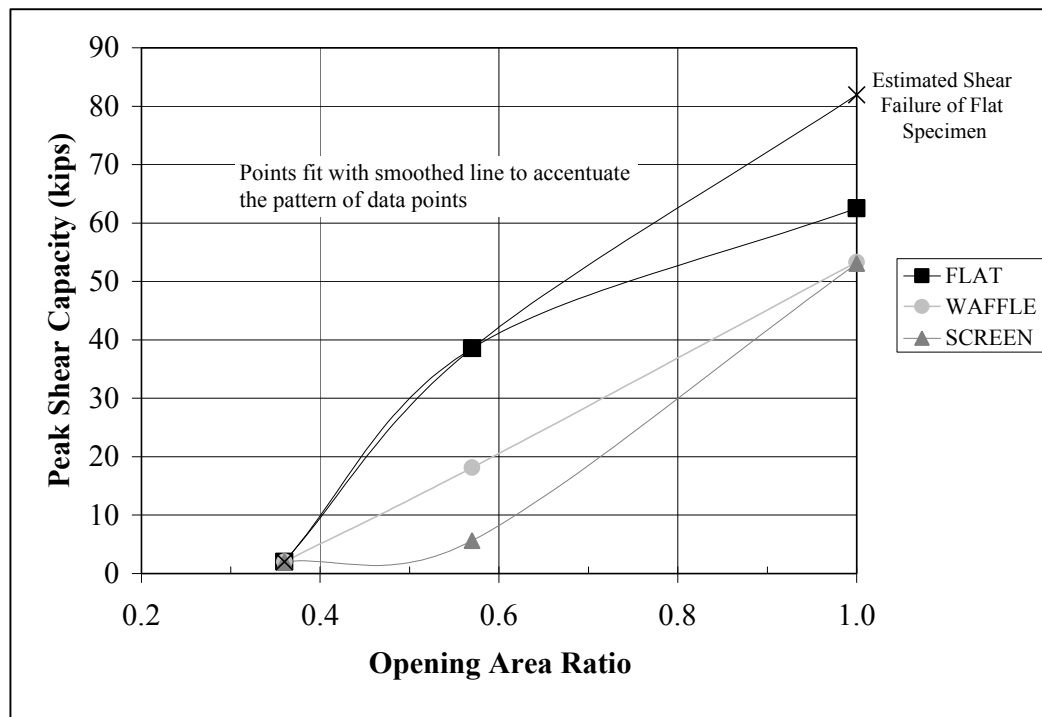


Figure 20  
Ultimate Capacity vs. Opening Area Ratio

Both the flat and waffle-grid specimens were fit with a smoothed curve to accentuate the pattern of the data points. These patterns, depicted in Figure 20, indicate that an empirical design approach is feasible with additional testing. A similar trend was not created for the screen-grid specimens since the Screen No. 2 specimen resulted in a questionable tested behavior. Additional testing should be done to confirm these findings and develop an accurate relationship for the screen-grid wall type.

Figure 20 also indicates that those wall specimens consisting of only full height wall segments of 2 ft (0.61 m) or less and with opening area ratios of about 0.4 or less should be designed as concrete moment frames. The reason for this is that as the number and size of openings increase, the height-to-length aspect ratio of the wall piers increase. The piers become cantilevers that are much more dependent on moment transfer through the collector and drag struts above and below openings to develop the overall wall (frame) shear resistance.

## **Design Methodology**

Although the effective wall thicknesses and empirical design approach show promise in improving the design of residential ICF walls with openings, the size of the test matrix requires that these preliminary findings should be confirmed before they are used in design. However, the use of Model 2 (i.e., wall segments with a 2:1 aspect ratio are dominated by shear and 4:1 aspect ratios are dominated by flexure) provides a conservative estimate of the shear capacity of the wall configurations when a wall segment with a 2:1 wall segment is present. Therefore the following design recommendations are suggested:

1. Use an analysis and design procedure that follows those used in Model 2, and
2. Only consider the area of the vertical cores in determining the shear capacity of walls with non-uniform cross sections. The actual wall width should be used when walls with uniform cross sections are being evaluated.

## **Conclusions**

The purpose of this research program was to evaluate the performance and predictability of concrete shear walls constructed with the three major ICFs used in residential construction: flat, waffle-grid, and screen-grid. A total of nine specimens were tested in the study. Cracks and other signs of damage were documented throughout the testing. Load and displacement data were recorded throughout the tests to provide insight into the behavior of the walls.

Overturning was a prevalent initial response to the loading history in all but one of the specimens (Screen No. 2). The degree of overturning varied with each specimen and was limited by the external hold-down restraint in order to evaluate the shear performance of the specimens.

Two models were used to estimate the shear capacity of the flat, waffle-grid, and screen-grid wall specimens. Model 1 for all wall types assumed all solid wall segments 2 ft (0.61 m) or greater in length act as a continuous solid wall to resist a concentrated lateral force at the top of the wall. Model 2 assumed that 2 ft (0.61 m) solid wall segments will be dominated by flexural behavior and that 4 ft (1.22 m) solid wall segments will be dominated by shear failure. Model 1 and Model

2 considered the rectangular cross sectional area of the flat specimens, but only the area of the vertical cores of the waffle-grid and screen-grid specimens in estimating the shear capacity. Model 2 was used to develop effective wall thicknesses for the waffle-grid and screen-grid wall specimens.

Model 1 and Model 2 provide conservative shear capacity estimates for specimens containing a full height segment dominated by shear behavior (i.e. height-to-length aspect ratio less than 2:1), with Model 1 providing a less conservative estimates than Model 2. This observation excludes the results from Screen No. 2 that is believed to be an anomalous result. Both of the models investigated did not provide a reasonable estimate for specimens containing only 2 ft (0.61 m) wall segments.

The effective wall thicknesses developed in this research closely coincides to those developed from the data published by PCA [13]. These thicknesses will allow the non-uniform cross sections to be analyzed as uniform cross sections. Additional testing should be conducted to confirm these results and develop effective wall thicknesses for additional non-uniform wall cross sections (i.e., 8 in (203.2 mm) waffle-grid).

An empirical method was investigated which relates the opening area ratio ( $r$ ) and unit shear capacity to the overall wall shear capacity. Equations were proposed for the flat and waffle-grid specimens to predict the effect of openings in wall lines of various configurations using an empirically derived relationship. The derived equations were linear with the flat specimens having a larger slope than that of the waffle-grid specimens. An equation was not derived for the screen-grid specimens since one of the three points was not reliable. With additional verification and development, this empirical based approach could prove to be a valuable design tool. However, this method may have its limitations when the opening area ratio decreases below 0.4 and specimens consist of only narrow wall segments (i.e. height-to-length ratios greater than 4:1). At this point, walls begin to behave more like moment frames (i.e., sway frames) than shear walls.

## Recommendations

Additional testing and analysis should be done to expand on the findings of this study. Future topics of study should include:

- Additional testing of shear walls with openings using the three major ICF systems. This work is needed to fully develop a simple and accurate the empirical method for predicting shear capacity based on the opening area ratio of concrete walls.
- Methods of accounting for shear contributions from narrow wall segments (i.e., greater than 2:1 aspect ratio) need to be improved for lightly reinforced and minimally detailed ICF walls.
- Walls should be tested using ASTM E564 procedures to better account for overturning failure modes. The effect of corner returns and dead loads should also be investigated in following a more realistic shear test method than the ASTM E72 method used in this report and commonly used by others.

## References

- [1] *Prescriptive Method for Insulating Concrete Forms in Residential Construction*, Prepared for the U.S. Department of Housing and Urban Development, the Portland Cement Association, and the National Association of Home Builders by the NAHB Research Center, Inc., Upper Marlboro, Maryland, 1998.
- [2] *International Residential Code (IRC)*, International Code Council, Reston, VA, 2000.
- [3] Elnashai, A.S., Pilakoutas, K., and Ambraseys, N.N., “Experimental Behavior of Reinforced Concrete Walls Under Earthquake Loading”, *Earthquake Engineering and Structural Dynamics*, Vol. 19, pp. 389-407, 1990.
- [4] Mau, S.T. and Hsu, T.C., “Shear Behavior of Reinforced Concrete Framed Wall Panels with Vertical Loads”, *ACI Structural Journal*, Vol. 84, No. 3, pp. 228-234, 1987.
- [5] Cardenas, A.E., Russel, H.G., and Corley, W.G., “Strength of Low Rise Structural Walls”, *Publication SP-63*, American Concrete Institute, Detroit, MI, 1980.
- [6] *Building Code Requirements for Reinforced Concrete (ACI 318-99)*, American Concrete Institute, Detroit, Michigan, 1999.
- [7] Osterle, R.G., Shiu, K.N., and Corley, W.G., “Web Crushing of Reinforced Concrete Structural Walls”, *ACI Journal*, Vol. 81, pp. 231-241, 1984.
- [8] *Uniform Building Code*, Vol. 2, International Council of Building Officials, Whittier, CA, 1997.
- [9] Taylor, C.P., Cote, P.A., and Wallace, J.W., “Design of Slender Reinforced Concrete Walls with Openings”, *ACI Structural Journal*, Vol. 95, No. 4, pp. 420-433, 1998.
- [10] Ali, A. and Wight, J.K., “Reinforced Structural Walls with Staggered Opening Configurations Under Reversed Cyclic Loading”, Report No. UMCE 90-05, Department of Civil Engineering, University of Michigan, Ann Arbor, MI, 1990.
- [11] Wallace, J.W., “New Methodology For Seismic Design of RC Shear Walls”, *Journal of Structural Engineering*, ASCE, Vol. 120, No. 3, 1994.
- [12] Lefas, I.D., Kotsovos, M.D., and Ambraseys, N.N., “Behavior of Reinforced Concrete Structural Walls: Strength, Deformation Characteristics, and Failure Mechanism”, *ACI Structural Journal*, Vol. 87, No. 1, pp. 23-31,
- [13] Mehrabi, A., “In-Plane Lateral Load Resistance of Wall Panels in Residential Buildings”, prepared for the Portland Cement Association by Construction Technology Laboratories, Inc., Skokie, IL, 1999.

- [14] *Standard for Hurricane Resistant Construction (SSTD 10-99)*, Southern Building Code Congress International, Birmingham, AL, 1999.
- [15] ASTM C143-96 *Slump of Portland Cement Concrete*, American Society of Testing Standards (ASTM), West Conshohocken, PA, 1996.
- [16] ASTM C39-96 *Standard Test Method for Compressive Strength of Cylindrical Concrete Specimens*, American Society of Testing and Materials (ASTM), West Conshohocken, PA, 1996.
- [17] ASTM C31-96 *Standard Practice for Making and Curing Concrete Test Specimens in the Field*, American Society of Testing and Materials (ASTM), West Conshohocken, PA, 1996.
- [18] ASTM C192-96 *Standard Practice for Making and Curing Concrete Test Specimens in the Laboratory*, American Society of Testing and Materials (ASTM), West Conshohocken, PA, 1996.
- [19] ASTM C78-94 *Standard Test Method for Flexural Strength of Concrete (Using Simple Beam with Third-Point Loading)*, American Society of Testing and Materials (ASTM), West Conshohocken, PA, 1994.
- [20] ASTM E72-95 *Construction Strength Tests of Panels for Building Construction*, American Society of Testing and Materials (ASTM), West Conshohocken, PA, 1995.
- [21] *Testing and Design of Lintels Using Insulating Concrete Forms*, Prepared for the U.S. Department of Housing and Urban Development, the Portland Cement Association, and the National Association of Home Builders by the NAHB Research Center, Inc., Upper Marlboro, Maryland, May 2000.
- [22] Sugiyama, H. and Yasumura, M., *Shear Properties of Plywood Sheathed Wall Panels with Openings*, Trans. of A.I.J., No. 338, 1984.
- [23] Sugiyama, H. and Matsumoto, T., *Empirical Equations for the Estimation of Racking Strength of a Plywood Sheathed Shear Wall with Openings*, Summary of Technical Papers Annual Meetings, Trans. of A.I.J., 1994.
- [24] Dolan, J. and Johnson, A., *Cyclic and Monotonic Tests of Long Shear Walls with Openings*, Prepared for the American Forest & Paper Association by Virginia Polytechnic Institute and State University, 1996.
- [25] Dolan, J. and Heine, C., *Monotonic Tests of Wood Frame Shear Walls with Various Openings and Base Restraint Configurations*, Prepared for the NAHB Research Center, Inc. by Virginia Polytechnic Institute and State University, 1997.

- [26] Dolan, J. and Heine, C., *Sequential Phased Displacement Cyclic Tests of Wood Frame Shear Walls with Various Openings and Base Restraint Configurations*, Prepared for the NAHB Research Center Inc. by Virginia Polytechnic Institute and State University, 1997.
- [27] Dolan, J. and Heine, C., *Sequential Phased Displacement Tests of Wood Framed Shear Walls with Corners*, Prepared for the NAHB Research Center, Inc. by Virginia Polytechnic Institute and State University, 1997.
- [28] *The Performance of Perforated Shear Walls with Narrow Wall Segments, Reduced Base Restraint, and Alternative Framing Methods*, Prepared for the U.S. Department of Housing and Urban Development and the National Association of Home Builders by the NAHB Research Center, Inc., Upper Marlboro, MD, 1998.
- [29] *Perforated Shear Walls with Conventional and Innovative Base Restraint Connections*, Prepared for the U.S. Department of Housing and Urban Development and the National Association of Home Builders by the NAHB Research Center, Inc., Upper Marlboro, MD, 1999.
- [30] *Shear and Diagonal Tension*, pt. 2, ACI-ASCE Committee 326, *ACI Journal*, Vol. 59, No. 2, February 1962, pp. 277-333.

## Appendix A – Example Calculations

The equations put forth in ACI represent an estimate such that 30 percent of the test data fell below the estimate. The test data was fit to a normal distribution and the coefficient of variation was 15.1 percent [30]. The predicted capacities in Table 10 – 14 were adjusted to mean estimates by multiplying the calculated values below by:

$$[1 - (F^{-1}(z)) * COV] = [1 - (F^{-1}(0.30)) * (0.151)] = [1 - (-0.52)(0.151)] = 1.08.$$

The above adjustment was done to provide relevant comparisons to the test data since the ACI Equations provide a 30-percent estimate.

### FLAT Wall Specimens

#### Flat No. 1: 1-4ft full height segment

##### MODEL 1 and MODEL 2

$$d = 44.0 \text{ in}$$

$$V_c = 2\sqrt{f'_c}hd = 2\sqrt{1,774 \text{ psi}}(6 \text{ in})(44.0 \text{ in}) = 22,239 \text{ lb}$$

$$P_u = 1.08(V_c) = 1.08(22,239 \text{ lb}) = 24,018 \text{ lb}$$

#### Flat No. 2: 1-4ft and 1-2ft full height segment

##### MODEL 1

$$d = 43.625 \text{ in} + 19.375 = 63.0 \text{ in}$$

$$V_c = 2\sqrt{f'_c}hd = 2\sqrt{1,774 \text{ psi}}(6 \text{ in})(63.0 \text{ in}) = 31,842 \text{ lb}$$

$$P_u = 1.08(V_c) = 1.08(31,842 \text{ lb}) = 34,389 \text{ lb}$$

##### MODEL 2

###### *4-ft segment*

$$d = 43.625 \text{ in}$$

$$V_c = 2\sqrt{f'_c}hd = 2\sqrt{1,774 \text{ psi}}(6 \text{ in})(43.625 \text{ in}) = 22,049 \text{ lb}$$

$$P_{u1} = 22,049 \text{ lb}$$

###### *2-ft segment*

$$a = \frac{A_s f_y}{0.85 f'_c b} = \frac{(0.20 \text{ in}^2)(60.9 \text{ ksi})}{0.85(1.774 \text{ ksi})(6 \text{ in})} = 1.346 \text{ in}$$

$$Z = d - a / 2 = (24 \text{ in} - 4.625 \text{ in}) - 1.346 \text{ in} / 2 = 18.702 \text{ in}$$

$$M_n = A_s f_y Z = (0.2 \text{ in}^2)(60.9 \text{ ksi})(18.702 \text{ in}) = 222.8 \text{ k-in}$$

$$P_{u2} = \frac{M_n}{l} = \frac{222.8 \text{ k-in}}{96 \text{ in}} (1000 \text{ lb / kip}) = 2,372 \text{ lb}$$

$$P_u = 1.08(P_{u1} + P_{u2}) = 1.08(22,049 \text{ lb} + 2,372 \text{ lb}) = 26,375 \text{ lb}$$

### Flat No. 3: 2-2ft full height segments

#### MODEL 1

$$d = 19.75in + 19.375in = 39.125in$$

$$V_c = 2\sqrt{f'_c}hd = 2\sqrt{1,774psi}(6in)(39.125in) = 19,775lb$$

$$P_u = 1.08(24,292lb) = 21,357lb$$

#### MODEL 2

*First 2-ft segment*

$$a = \frac{A_s f_y}{0.85 f'_c b} = \frac{(0.20in^2)(60.9ksi)}{0.85(1.774ksi)(6in)} = 1.346in$$

$$Z = d - a/2 = (24in - 4.625in) - 1.346in/2 = 18.702in$$

$$M_n = A_s f_y Z = (0.2in^2)(60.9ksi)(18.702in) = 227.8k - in$$

$$P_{u1} = \frac{M_n}{l} = \frac{227.8k - in}{96in} (1000lb / kip) = 2,372lb$$

*Second 2-ft segment*

$$a = \frac{A_s f_y}{0.85 f'_c b} = \frac{(0.20in^2)(60.9ksi)}{0.85(1.774ksi)(6in)} = 1.346in$$

$$Z = d - a/2 = (24in - 4.25in) - 1.346in/2 = 19.077in$$

$$M_n = A_s f_y Z = (0.2in^2)(60.9ksi)(19.077in) = 232.4k - in$$

$$P_{u2} = \frac{M_n}{l} = \frac{232.4k - ft}{96ft} (1000lb / kip) = 2,421lb$$

$$P_u = 1.08(P_{u1} + P_{u2}) = 1.08(2,372lb + 2,421lb) = 5,176lb$$

## WAFFLE-GRID Wall Specimens

### Waffle No. 1: 1-4ft full height segment

#### MODEL 1 and MODEL 2

$$V_{c-core} = 2\sqrt{f'_c}hd = 2\sqrt{1,774\text{psi}}(5\text{in})(6.25\text{in}/\text{core}) = 2,632\text{lb}/\text{core}$$

$$P_u = 1.08(3.5\text{cores})(2,632\text{lb}/\text{core}) = 9,949\text{lb}$$

#### MODEL 2 – Effective Thickness

$$d = 43.75\text{in}$$

$$V_{equiv} = 2\sqrt{f'_c}hd = 2\sqrt{1,774\text{psi}}(43.75\text{in})h = (3,685\text{lb}/\text{in})h$$

$$P_u = 1.08(3,685\text{lb}/\text{in})h = 17,770\text{lb} \Rightarrow h = 4.46\text{in}$$

### Waffle No. 2: 1-4ft and 1-2ft full height segment

#### MODEL 1

$$V_{c-core} = 2\sqrt{f'_c}hd = 2\sqrt{1,774\text{psi}}(5\text{in})(6.25\text{in}/\text{core}) = 2,632\text{lb}/\text{core}$$

$$P_u = 1.08(5.0\text{cores})(2,632\text{lb}/\text{core}) = 14,212\text{lb}$$

#### MODEL 2

##### *4-ft segment*

$$V_{c-core} = 2\sqrt{f'_c}hd = 2\sqrt{1,774\text{psi}}(5\text{in})(6.25\text{in}/\text{core}) = 2,632\text{lb}/\text{core}$$

$$P_{u1} = (3.5\text{cores})(2,632\text{lb}/\text{core}) = 9,212\text{lb}$$

##### *2-ft segment*

$$a = \frac{A_s f_y}{0.85 f'_c b} = \frac{(0.20\text{in}^2)(60.9\text{ksi})}{0.85(1.774\text{ksi})(5\text{in})} = 1.615\text{in}$$

$$Z = d - a / 2 = (24\text{in} - 4.5\text{in}) - 1.615\text{in} / 2 = 18.693\text{in}$$

$$M_n = A_s f_y Z = (0.2\text{in}^2)(60.9\text{ksi})(18.693\text{in}) = 227.7\text{k} - \text{in}$$

$$P_{u2} = \frac{M_n}{l} = \frac{227.7\text{k} - \text{in}}{96\text{in}} (1000\text{lb}/\text{kip}) = 2,372\text{lb}$$

$$P_u = 1.08(P_{u1} + P_{u2}) = 1.08(9,212\text{lb} + 2,372\text{lb}) = 12,511\text{lb}$$

#### MODEL 2 – Effective Thickness

##### *4-ft segment*

$$d = 43.5\text{in}$$

$$V_{equiv} = 2\sqrt{f'_c}hd = 2\sqrt{1,774\text{psi}}(43.5\text{in})h = (3,664\text{lb}/\text{in})h$$

$$P_{u1} = (3,664\text{lb}/\text{in})h$$

*2-ft segment*

$$a = \frac{A_s f_y}{0.85 f'_c h} = \frac{(0.20 \text{ in}^2)(60.9 \text{ ksi})}{0.85(1.774 \text{ ksi})h} = (8.077 / h) \text{ in}$$

$$Z = d - a / 2 = (24 \text{ in} - 4.5 \text{ in}) - (8.077 / h) \text{ in} / 2 = 19.5 \text{ in} - (4.039 / h) \text{ in}$$

$$M_n = A_s f_y Z = (0.20 \text{ in}^2)(60.9 \text{ ksi})(19.5 \text{ in} - (4.039 / h) \text{ in}) = 237.5 \text{ k} \cdot \text{in} - (49.19 / h) \text{ k} \cdot \text{in}$$

$$P_{u2} = \frac{M_n}{l} = \frac{237.5 \text{ k} \cdot \text{in} - (49.19 / h) \text{ k} \cdot \text{in}}{96 \text{ in}} (1000 \text{ lb} / \text{kip}) = 2,274 \text{ lb} - (512.4 / h) \text{ lb}$$

$$P_u = P_{u1} + P_{u2} = 1.08((3,664)h + 2,274 - (512.4 / h)) = 18,110 \Rightarrow h = 3.99 \text{ in}$$

### **Waffle No. 3: 2-2ft full height segments**

#### MODEL 1

$$V_{c-core} = 2\sqrt{f'_c} h d = 2\sqrt{1,774 \text{ psi}}(5 \text{ in})(6.25 \text{ in} / \text{core}) = 2,632 \text{ lb} / \text{core}$$

$$P_u = 1.08(3.0 \text{ cores})(2,632 \text{ lb} / \text{core}) = 8,527 \text{ lb}$$

#### MODEL 2

*Both 2-ft segments*

$$a = \frac{A_s f_y}{0.85 f'_c b} = \frac{(0.20 \text{ in}^2)(60.9 \text{ ksi})}{0.85(1.774 \text{ ksi})(5 \text{ in})} = 1.615 \text{ in}$$

$$Z = d - a / 2 = (24 \text{ in} - 4.625 \text{ in}) - 1.615 \text{ in} / 2 = 18.568 \text{ in}$$

$$M_n = A_s f_y Z = (0.20 \text{ in}^2)(60.9 \text{ ksi})(18.568 \text{ in}) = 226.2 \text{ k} - \text{in}$$

$$P_{u1} = \frac{M_n}{l} = \frac{226.2 \text{ k} - \text{in}}{96 \text{ in}} (1000 \text{ lb} / \text{kip}) = 2,356 \text{ lb}$$

$$P_u = 1.08(2)(P_{u1}) = 1.08(2)(2,356 \text{ lb}) = 5,089 \text{ lb}$$

## SCREEN-GRID Wall Specimens

### Screen No. 1: 1-4ft full height segment

#### MODEL 1 and MODEL 2

$$V_{c-core} = 2\sqrt{f'_c}hd = 2\sqrt{1,774\text{psi}}(5\text{in})(5\text{in / core}) = 2,106\text{lb / core}$$

$$P_u = 1.08(4.5\text{cores})(2,106\text{lb / core}) = 10,235\text{lb}$$

#### MODEL 2 – Effective Thickness

$$d = 44.0\text{in}$$

$$V_{equiv} = 2\sqrt{f'_c}hd = 2\sqrt{1,774\text{psi}}(44.0\text{in})h = (3,706h)\text{lb}$$

$$P_u = 1.08(3,706h)\text{lb} = 17,690\text{lb} \Rightarrow h = 4.42\text{in}$$

### Screen No. 2: 1-4ft and 1-2ft full height segment

#### MODEL 1

$$V_{c-core} = 2\sqrt{f'_c}hd = 2\sqrt{1,774\text{psi}}(5\text{in})(5\text{in / core}) = 2,106\text{lb / core}$$

$$P_u = 1.08(7\text{cores})(2,106\text{lb / core}) = 15,921\text{lb}$$

#### MODEL 2

##### *4-ft segment*

$$V_{c-core} = 2\sqrt{f'_c}hd = 2\sqrt{1,774\text{psi}}(5\text{in})(5\text{in / core}) = 2,106\text{lb / core}$$

$$P_{u1} = 4.5\text{cores}(2,106\text{lb / core}) = 9,477\text{lb}$$

##### *2-ft segment*

$$a = \frac{A_s f_y}{0.85 f'_c b} = \frac{(0.20\text{in}^2)(60.9\text{ksi})}{0.85(1.774\text{ksi})(5\text{in})} = 1.615\text{in}$$

$$Z = d - a / 2 = (24\text{in} - 2\text{in}) - 1.615\text{in} / 2 = 21.193\text{in}$$

$$M_n = A_s f_y Z = (0.2\text{in}^2)(60.9\text{ksi})(21.193\text{in}) = 258.1\text{k} - \text{in}$$

$$P_{u2} = \frac{M_n}{h} = \frac{258.1\text{k} - \text{in}}{96\text{in}} (1000\text{lb / kip}) = 2,689\text{lb}$$

$$P_u = 1.08(P_{u1} + P_{u2}) = 1.08(9,477\text{lb} + 2,689\text{lb}) = 13,139\text{lb}$$

#### MODEL 2 – Effective Thickness

##### *4-ft segment*

$$d = 43.75\text{in}$$

$$V_{equiv} = 2\sqrt{f'_c}hd = 2\sqrt{1,774\text{psi}}(43.75\text{in})h = 3,685h$$

$$P_{u1} = 3,685h$$

*2-ft segment*

$$a = \frac{A_s f_y}{0.85 f'_c h} = \frac{(0.20 \text{ in}^2)(60.9 \text{ ksi})}{0.85(1.774 \text{ ksi})h} = 8.077 / h$$

$$Z = d - a / 2 = (24 \text{ in} - 2 \text{ in}) - (8.077 / h) / 2 = 22 \text{ in} - (4.039 / h) \text{ in}$$

$$M_n = A_s f_y Z = (0.20 \text{ in}^2)(60.9 \text{ ksi})(22 \text{ in} - (4.039 / h) \text{ in}) = 267.96 k \cdot \text{in} - (49.192 / h) k \cdot \text{in}$$

$$P_{u2} = \frac{M_n}{l} = \frac{267.96 k \cdot \text{in} - (49.192 / h) k \cdot \text{in}}{96 \text{ in}} (1000 \text{ lb} / \text{kip}) = 2,791 \text{ lb} - (512.4 / h) \text{ lb}$$

$$P_u = P_{u1} + P_{u2} = 1.08(3,685 h + 2,791 - 512.4 / h) = 5,630 \text{ lb} \Rightarrow h = 0.82 \text{ in}$$

### Screen No. 3: 2-2ft full height segments

#### MODEL 1

$$V_{c-\text{core}} = 2\sqrt{f'_c} h d = 2\sqrt{1,774 \text{ psi}}(5 \text{ in})(5 \text{ in} / \text{core}) = 2,106 \text{ lb} / \text{core}$$

$$P_u = 1.08(4 \text{ cores})(2,106 \text{ lb} / \text{core}) = 9,098 \text{ lb}$$

#### MODEL 2

*One 2-ft segment*

$$a = \frac{A_s f_y}{0.85 f'_c b} = \frac{(0.20 \text{ in}^2)(60.9 \text{ ksi})}{0.85(1.774 \text{ ksi})(5 \text{ in})} = 1.615 \text{ in}$$

$$Z = d - a / 2 = (24 \text{ in} - 2.5 \text{ in}) - 1.615 \text{ in} / 2 = 20.693 \text{ in}$$

$$M_n = A_s f_y Z = (0.20 \text{ in}^2)(60.9 \text{ ksi})(20.693 \text{ in}) = 252.0 k - \text{in}$$

$$P_{u1} = \frac{M_n}{h} = \frac{252.0 k - \text{in}}{96 \text{ in}} (1000 \text{ lb} / \text{kip}) = 2,625 \text{ lb}$$

*Second 2-ft segment*

$$a = \frac{A_s f_y}{0.85 f'_c b} = \frac{(0.20 \text{ in}^2)(60.9 \text{ ksi})}{0.85(1.774 \text{ ksi})(5 \text{ in})} = 1.615 \text{ in}$$

$$Z = d - a / 2 = (24 \text{ in} - 1.5 \text{ in}) - 1.615 \text{ in} / 2 = 21.693 \text{ in}$$

$$M_n = A_s f_y Z = (0.20 \text{ in}^2)(60.9 \text{ ksi})(21.693 \text{ in}) = 264.2 k - \text{in}$$

$$P_{u2} = \frac{M_n}{h} = \frac{264.2 k - \text{in}}{96 \text{ in}} (1000 \text{ lb} / \text{kip}) = 2,752 \text{ lb}$$

$$P_u = 1.08(P_{u1} + P_{u2}) = 1.08(2,625 \text{ lb} + 2,752 \text{ lb}) = 5,807 \text{ lb}$$